Journal of Petroleum Science and Engineering 205 (2021) 108943

Contents lists available at ScienceDirect

Journal of Petroleum Science and Engineering

journal homepage: www.elsevier.com/locate/petrol

Migration and accumulation of crude oils in the Qionghai Uplift, Pearl River Mouth Basin, Offshore South China Sea

Guangjie Xie [a,b], Dongxia Chen [a,b,*], Lu Chang [c], Jinheng Li [a,b], Zhijun Yin [a,b]

[a] State Key Laboratory of Petroleum Resources and Prospecting, China University of Petroleum, Beijing, 102249, China
[b] College of Geosciences, China University of Petroleum, Beijing, 102249, China
[c] Shaanxi Energy Institute, Xianyang, 712000, China

ARTICLE INFO

Keywords:
Qionghai uplift
Zhu III super-depression
Oil–source correlation
Migration conduit
Hydrocarbon accumulation

ABSTRACT

The crude oils migration and accumulation of the Qionghai (QH) Uplift in the Zhu III Super-depression was investigated from the perspective of oil source and migration conduit using gas chromatography-mass spectrometry (GC-MS), stable carbon isotope, quantitative grain fluorescence (QGF) analysis and basin simulation methods. The results on the oil-source correlation showed that oil origins of the five typical reservoirs were very complicated. Crude oils of the eastern and western parts of the QH Uplift were from the Wenchang A sag and the Wenchang B sag, respectively, whereas oil sources of the central part of the QH Uplift were from both the Wenchang A and B sags. The research on the migration conduit showed that structure ridge, fault and connectivity sand body jointly controlled crude oil migration and accumulation in the study area. Under the control of structure ridges and well-connected sand bodies, crude oils accumulated at a low-magnitude folding structure forming the WC13-1, WC13-2 and QH18-1 reservoirs, whereas the sealed fault played an important role in forming the WC8-3 and WC13-6 reservoirs. Combing the differences in oil origins and crude oils migration conduits, we finally identified two types of crude oils migration and accumulation modes from the Wenchang Sag to the QH Uplift. One was a gentle-slope long-distance migration and accumulation model, which was developed from the Wenchang A sag to the QH Uplift. The other was a steep-slope short-distance migration and accumulation model, which was developed from the Wenchang B sag to the QH Uplift. This study could provide guidance for exploring the petroleum potential and prospecting promising zones in the South China Sea.

1. Introduction

The Zhu III Super-depression, mainly including six structural divisions, is located at the western Pearl River Mouth Basin (PRMB) and has experienced more than 30 years of hydrocarbon exploration history (Zhang et al., 2011b). The Wenchang A and B sags and the QH Uplift are the main objectives of petroleum exploration and development. Crude oil reserves and natural gas reserves are over 1.5×10^8 m^3 and 400×10^8 m^3, respectively (Zhong et al., 2018; Li et al., 2020). Particularly, it has been discovered that the QH Uplift, with oil reservoirs such as the WC8-3, the WC13-1, the QH18-1 and so on, is the main hydrocarbon exploration and development area in the Zhu III Super-depression (Gong et al., 2004). Both of the Oligocene Enping Formation (E_3e) and the Eocene Wenchang Formation (E_2w) are rich in hydrocarbon source rocks in the Wenchang A and B sags (Quan et al., 2017). However, the QH Uplift lacks the Wenchang Formation and the Enping Formation, and thus it does not have the capacity to generate hydrocarbons (Gan et al., 2014a). There is controversy about the specific source of crude oil in the QH Uplift originating from the Wenchang A or B sags, or both (A and B sags) (Gong et al., 2004). Many scholars have also drawn different conclusions on the hydrocarbon transmission system of the QH Uplift (Jiang and Zhou, 1998; Jiang et al., 2009; Xu et al., 2010). For example, Xu et al. (2000) believed that the inherited tectonic ridge is a favourable conduit for hydrocarbon migration by analysing the maturity of crude oil and nitrogen compounds from the Wenchang A sag. J.L. Li et al. (2015) proposed that crude oils from the Wenchang B sag accumulating in the QH Uplift anticline trap are dominated by lateral migration along the combination of the sandstone skeleton and fault.

The above views were based on hydrocarbon migration with a single oil source, but different opinion is put forward in this paper now. Therefore, this paper is based on oil-source correlation and carefully discusses crude oil migration and accumulation of the QH Uplift by

* Corresponding author. State Key Laboratory of Petroleum Resources and Prospecting, China University of Petroleum, Beijing 102249, China.
E-mail address: lindachen@cup.edu.cn (D. Chen).

https://doi.org/10.1016/j.petrol.2021.108943
Received 14 April 2020; Received in revised form 18 February 2021; Accepted 12 May 2021
Available online 19 May 2021

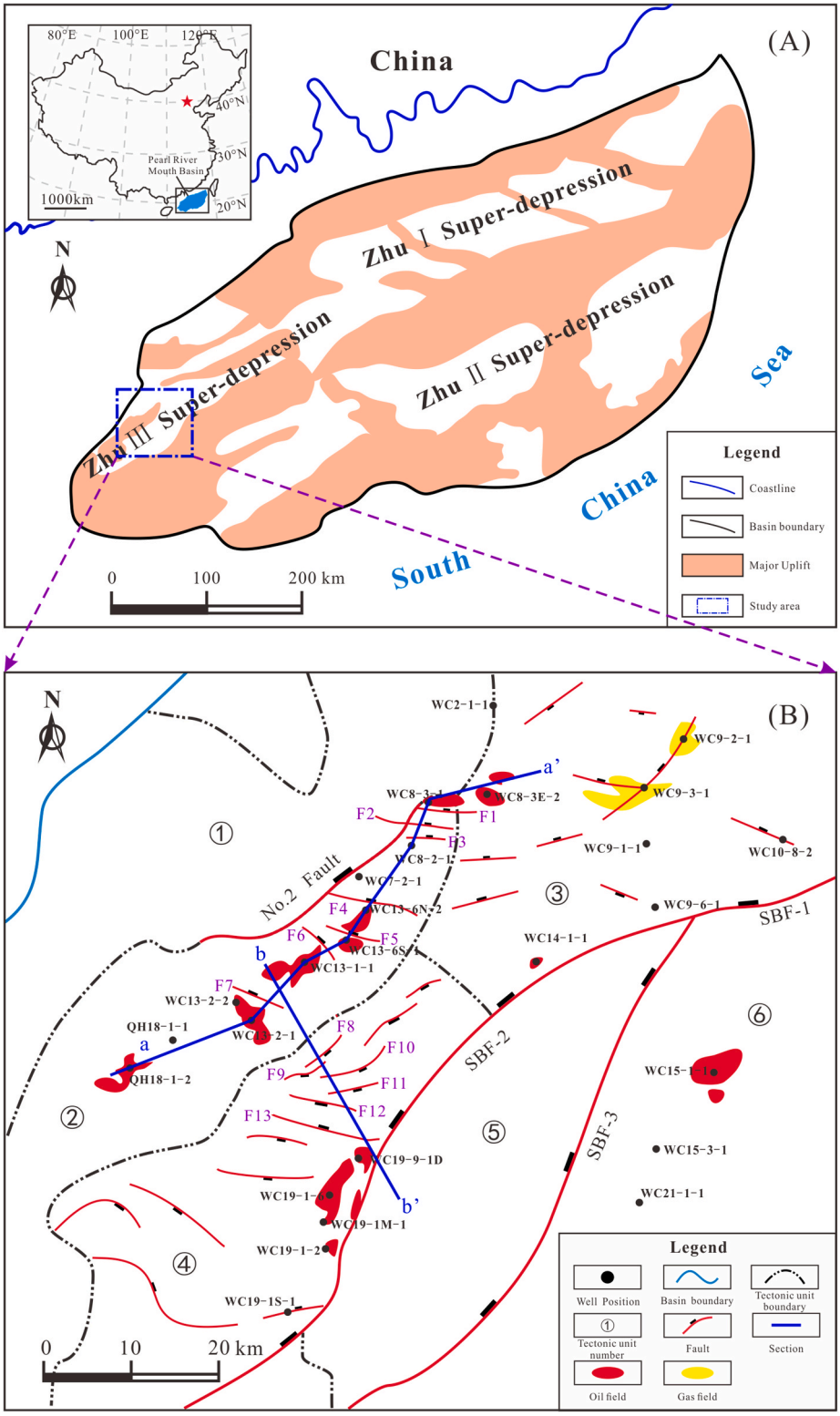

Fig. 1. (A) Map showing the structural divisions of the Pearl River Mouth Basin, China, and location of the Zhu III Super-depression (modified from Zhu and Mi, 2011). (B) Map showing structural units of Zhu III Super-depression: ① Qionghai Sag; ② Qionghai Uplift; ③ Wenchang A sag; ④ Wenchang B sag; ⑤ Wenchang C sag; ⑥ Shenhu Uplift. Sampled wells, important faults (F1~F13), typical sections (aa' and bb') and hydrocarbon shows (modified from Zhang et al., 2014; Quan et al., 2017). SBF=South Boundary Fault.

taking oil reservoir as a unit and breaking the thinking of single source controlling oil accumulation. According to analysis of the characteristics of oil fields in the QH Uplift, it is suggested that the oil origins of the QH Uplift (divided into three parts according to orientation, i.e., east, middle and west) may be very complicated and that it is not as simple as a mixed oil source. Therefore, analysis of the oil sources is critical to the establishment of crude oil migration and accumulation models. With hydrocarbon exploration progress and technology advancement, the more accurate understanding of the oil source and the transmission system can be achieved.

Gas chromatography-mass spectrometry (GC-MS), quantitative grain fluorescence (QGF) and quantitative grain fluorescence on extract (QGF-E) analyses, stable carbon isotope analysis and a basin simulation model were used to numerically identify the origin of crude oils, to simulate hydrocarbon migration paths and to comprehensively analyse the crude oil migration and accumulation. We found the key factors controlling

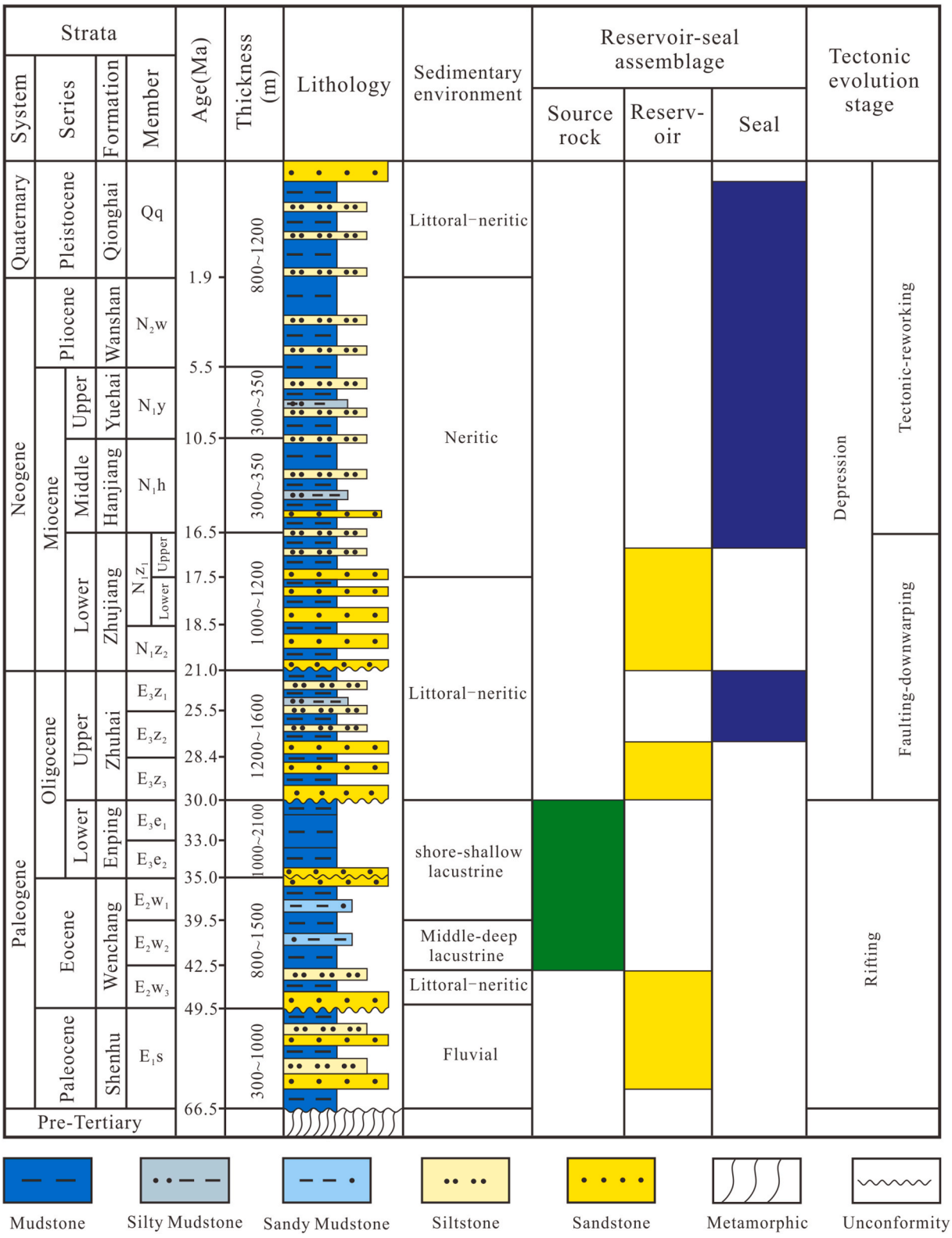

Fig. 2. Stratigraphic synthesis column, reservoir-seal assemblage and tectonic evolution stage of Zhu III Super-depression (modified from Jiang et al., 2008; Li and Chen et al., 2014).

crude oil migration were structure ridge, fault and sand body connectivity. Integrating an accurate crude oil migration and accumulation model would be used to predict the favourable area for crude oil accumulation and design the wildcat wells. The main purpose was to gain a deep understanding on crude oils accumulation of the QH Uplift and its surroundings, and provide an improved understanding of petroleum potential of the low-exploration and mature areas in South China Sea.

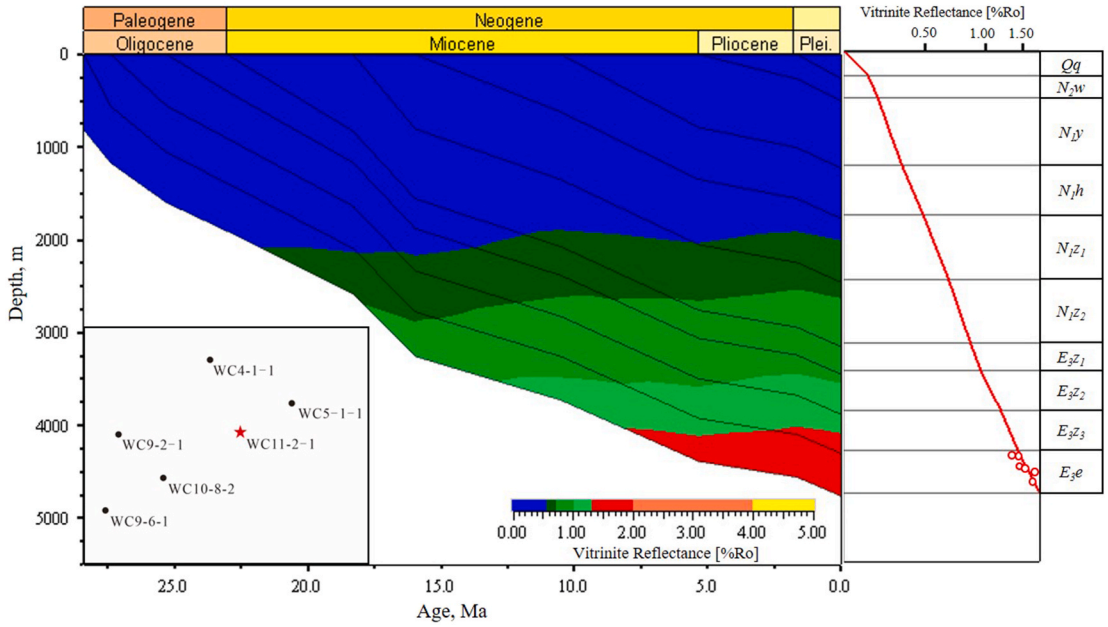

Fig. 3. The burial history and maturity evolution of Well WC11-2-1 in the Wenchang A sag.

2. Geological setting

The Pearl River Mouth Basin (Fig. 1A), a Cenozoic continental marginal extension basin mainly developed above the pre-Tertiary basement, is located at the eastern coastal waters of continental shelf in the northern South China Sea (Shi et al., 2015). The Zhu III Super-depression is a key area for hydrocarbon exploration and development in the western of PRMB and has achieved some major breakthroughs, such as the QH Uplift (He and Liu et al., 2008). The QH Uplift (Fig. 1B), with an area of 1420 km^2, adjoins the QH sag, Wenchang A sag and Wenchang B sag in the north, northeast and southeast, respectively (You et al., 2011). Because of the control of stretching and the influence of right-lateral strike–slip after Pre-Tertiary, there have been three tectonic evolution stages in the Zhu III Super-depression (Fig. 2): Rifting, Faulting-down-warping and Tectonic-reworking, respectively, forming six structural divisions in the Zhu III Super-depression, especially the QH Uplift and the Wenchang A and B sags (Gan et al., 2014a; Li et al., 2020). The long axis direction of the Wenchang A and B sags is roughly NE-SW, and Zhu III Super-depression appears as a typical skip-shaped fault depression, as does the Wenchang Sag (Li et al., 2010, 2015; H. Li et al., 2015).

The QH Uplift, lacking the E_2w Formation and the E_3e Formation, is mainly covered by the Neogene strata (Fig. 2), a littoral–neritic sedimentary environment, and the Miocene Zhujiang Formation (N_1z) is a good reservoir (Cheng, 2013; Zhang and Zhu et al., 2015). However, source rocks, the E_3e and E_2w Formation, widely developed in the Wenchang Sag (A and B sags), can provide enough hydrocarbons for the reservoirs of the QH Uplift (Zhang et al., 2009). We also find that the slope of the Wenchang A sag to the Uplift is gentler than that of the Wenchang B sag to the Uplift. So far, many oil fields or oil-bearing structures, such as WC13-1, WC13-2, WC13-6 and QH18-1, have been discovered in the QH Uplift (Xie, 2011), resulting in an annual production of crude oil of over 200 × 10^4 m^3 (Gan et al., 2014b).

3. Data and method

3.1. Data

About 37 crude oil samples from eighteen (18) wells in the QH Uplift were used in GC-MS analysis and stable carbon isotope analysis. 143 rock samples of 46 wells in the QH Uplift and the Wenchang Sag, with 35 and 108 samples from the cores and cuttings (including mudstone and sandstone cuttings), respectively, were selected for GC-MS, QGF and QGF-E analyses. Seventeen (17) wells and eight (8) sections, thermal evolution of source rock, were simulated by PetroMod® Software, and Trinity® Software was used to simulate the hydrocarbon migration pathway of 3D structural surfaces.

3.2. Methods

3.2.1. GC-MS analysis

The oil–source rock correlation would be effectively determined by GC-MS analysis. GC retention times and mass spectra (MS) comparison could effectively identify compounds, relatively quantified by integral areas of their peaks (Li and Xing et al., 2018). Analyses of the saturated hydrocarbon fractions were carried out on an Agilent 5975i mass spectrometer coupled to an Agilent 6890 gas chromatograph equipped with an HP-5MS capillary column (30 m × 0.25 mm × 0.25 μm film thickness). The MS was operated in both full-scan and selected ion monitoring (SIM) modes with an electron ionization mode at 70 eV. Helium was usually selected as carrier gas and its constant flow was set to 1 cm^3/min in this study (S.M. Li et al., 2010). The GC oven temperature was initially set at 50 °C with a holding time of 1min and programmed to 120 °C at 20 °C/min, then to 310 °C at 3 °C/min with a final holding time of 10min.

3.2.2. QGF and QGF-E analyses

QGF method could be used to determine paleo-oil zones, utilizing fluorescence spectrophotometry, as well as would provide some basis for identifying hydrocarbon migration, whereas the QGF-E method could be mainly used to identify current (residual) oil (Wang and Zeng et al., 2017; Wang et al., 2018). QGF could measure fluorescence emission spectra, with a wavelength of 300 nm and 600 nm, when cleaned reservoir grains were exposed to ultraviolet (UV) light. QGF Index was defined as the average spectral intensity between 375 nm and 475 nm normalized to the spectral intensity at 300 nm and responded to paleo-oil saturation. QGF Index values measured from paleo-oil samples were usually more than 4, whereas samples would be explained as water-bearing zones when QGF Index values were less than 4 (Liu et al., 2007; Liu and George et al., 2014). QGF-E analysis was based on the

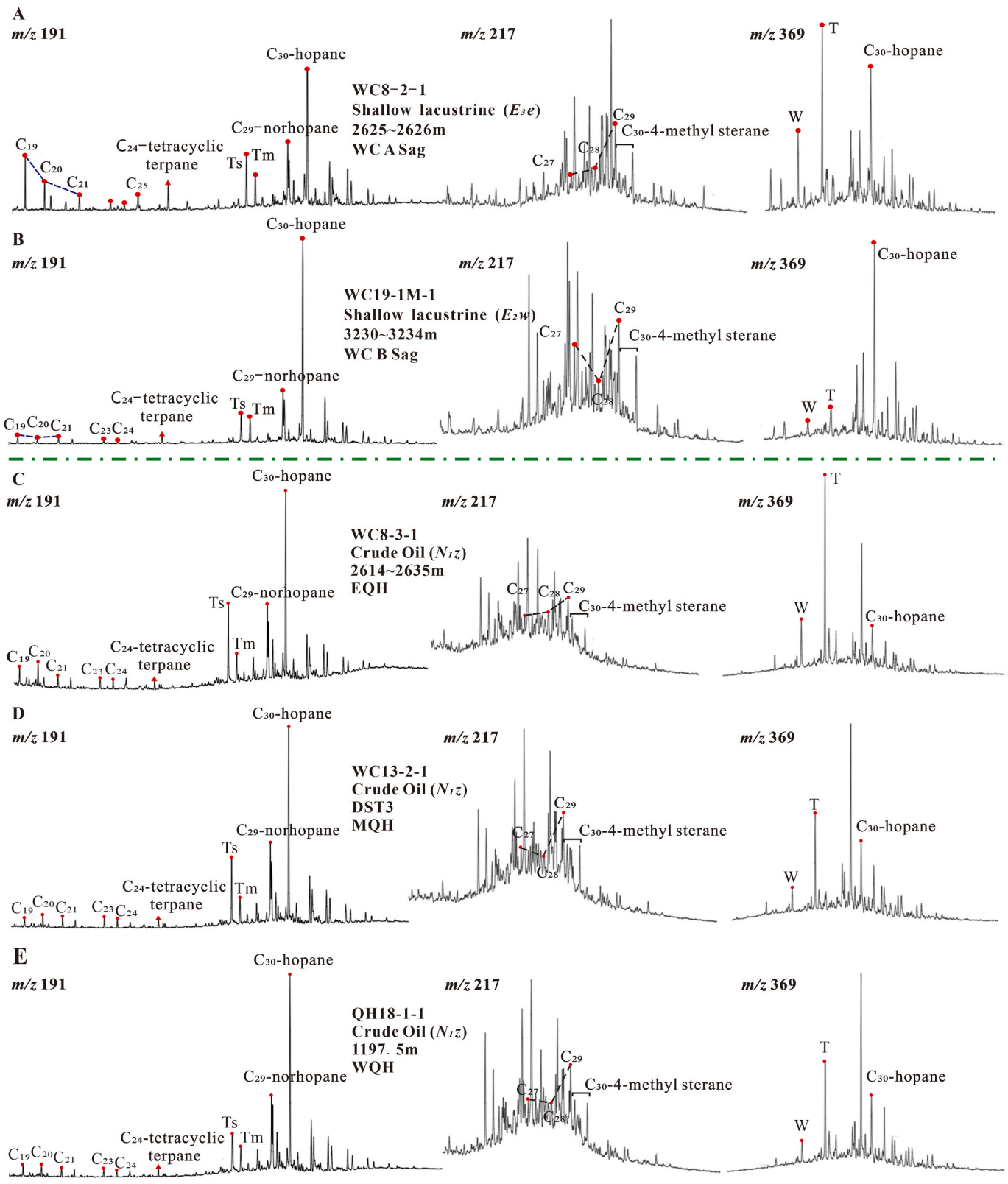

Fig. 4. m/z 191, 217 and 369 Mass fragmentograms of typical source rocks (A and B) in the Wenchang Sag and crude oils (C, D and E) from typical reservoirs of the QH Uplift, showing different biomarker characteristics. WC A sag: Wenchang A sag; WC B sag: Wenchang B sag; EQH: the east part of the QH Uplift; MQH: the middle part of the QH Uplift; WQH: the west part of the QH Uplift; N_1z: Zhujiang Formation; E_3e: Enping Formation; E_2w: Wenchang Formation; Ts: C_{27}-17α(H)-Trisnorhopane; Tm: C_{27}-18α(H)-Trisnorhopane; 'C_{27}' & 'C_{28}' & 'C_{29}': regular steranes; 'W' & 'T': bicadinanes).

Table 1
Main geochemical parameters in the Wenchang Sag and the QH Uplift.

Area	Well Name	Depth, m	Strata	$\delta^{13}C$‰, PDB	Pr/Ph	C30-4-methyl sterane
WC A Sag	WC9-6-1	3776–3784	E_3e	−29.16	3.83	0.18
		3818–3822	E_3e	−29.13	5.31	0.19
	WC11-2-1	4372–4376	E_3e	−28.94	4.13	0.14
		4432	E_3e	−28.59	3.89	0.18
		4516–4520	E_3e	−29.10	2.56	0.12
		4588–4592	E_3e	−28.35	5.05	0.16
WC B Sag	WC19–1N-1	2402–2408	E_3e	−26.89	5.90	0.12
		2562–2566	E_3e	−27.23	7.99	0.05
	WC19-1M-1	2590–2594	E_3e	−26.64	8.62	0.03
		2888–2896	E_3e	−26.48	6.79	0.10
		3070–3072	E_2w_1	−27.61	3.30	0.23
		3230–3234	E_2w_1	−27.16	3.24	0.33
	WC19-1-2	2805–2820	E_2w_1	−26.38	3.11	0.29
		3240–3242	E_2w_1	−26.02	2.30	0.28
	WC19-1M-1	3256–3258	E_2w_2	−23.96	2.01	0.35
		3304–3310	E_2w_2	−23.92	1.91	0.56
		3334–3342	E_2w_2	−24.21	1.30	0.36
		3368–3376	E_2w_2	−23.76	1.80	0.39
		3392–3394	E_2w_2	−23.39	1.84	0.58
East of QH Uplift	WC8-3-1	2614–3635	N_1z	−29.20	4.79	0.14
	WC8-3E-1	1699–1700	N_1z	−29.40	2.60	0.22
	WC8-3E-2	1666–1694	N_1z	−29.40	3.24	0.18
	WC13–6N-1	1283–1350	N_1z	−29.10	3.40	0.22
	WC13–6N-2	1400–1409	N_1z	−29.00	4.30	0.25
Middle of QH Uplift	WC13–1S-1	1247.1	N_1z	−28.30	3.35	0.23
	WC13-1-2	1400–1410	N_1z	−28.40	4.10	0.26
	WC13-1-1	1385–1402	N_1z	−27.50	3.76	0.20
	WC13-2-1	1206–1216	N_1z	−27.30	3.03	0.23
	WC13-2-2	1106	N_1z	−28.30	3.52	0.25
		1180–1190	N_1z	−26.80	3.10	0.21
West of QH Uplift	QH18-1-1	1205.4	N_1z	−26.30	2.84	0.27
	QH18-1-2	1292–1302	N_1z	−26.50	2.67	0.28

samples of QGF analysis and then fluorescence intensities of the extractive fluid were achieved.

3.2.3. Stable carbon isotope analysis

It was performed on a FLASH HT EA-MAT 253 IRMS instrument. N-alkanes in the samples were isolated from the saturated hydrocarbon fractions with 5 Å molecular sieves (Wang et al., 2018). Helium was usually selected as carrier gas and its constant flow was set to 100 cm^3/min in this study. Its reaction furnace temperature was initially set to 980 °C and then adjusted according to actual situation. The reactor packing was generally chromium oxide, cobalt oxide and others (Sun et al., 2019). All isotopic values were reported as $\delta^{13}C$ (‰) relative to Vienna Pee Dee Belemnite standard (V-PDB) and corrected for ^{17}O contribution.

3.2.4. Basin simulation

The PetroMod® Software was a comprehensive tool in basin simulation, such as hydrocarbon generation and migration, because it could carry out seismic, stratigraphic and geological interpretations, and consider thermal, fluid-flow data into multidimensional simulations in sedimentary basins (He and Graham et al., 2014; Piero et al., 2016). Additionally, the Trinity® Software developed by Zetaware (USA) used a fast algorithm to calculate the 'migration path' based on the geometry of the structure; it also considered the effects of pressure and capillary forces on the migration path represented by the streamline. The basic principle of the algorithm was that the direction of hydrocarbon migration was consistent with the direction of the reduction of the combined force of buoyancy, pressure and capillary pressure (Pepper et al., 1995).

4. Results and discussion

4.1. Origin of crude oils

There are two hydrocarbon-rich depressions, the Wenchang A and B sags, and there are two source rocks developed in each depression, namely, the Wenchang Formation (E_2w) and the Enping Formation (E_3e), respectively (Fu et al., 2011; Zhu et al., 2013). But main source rock in each depression is different (Quan et al., 2017). Previous studies

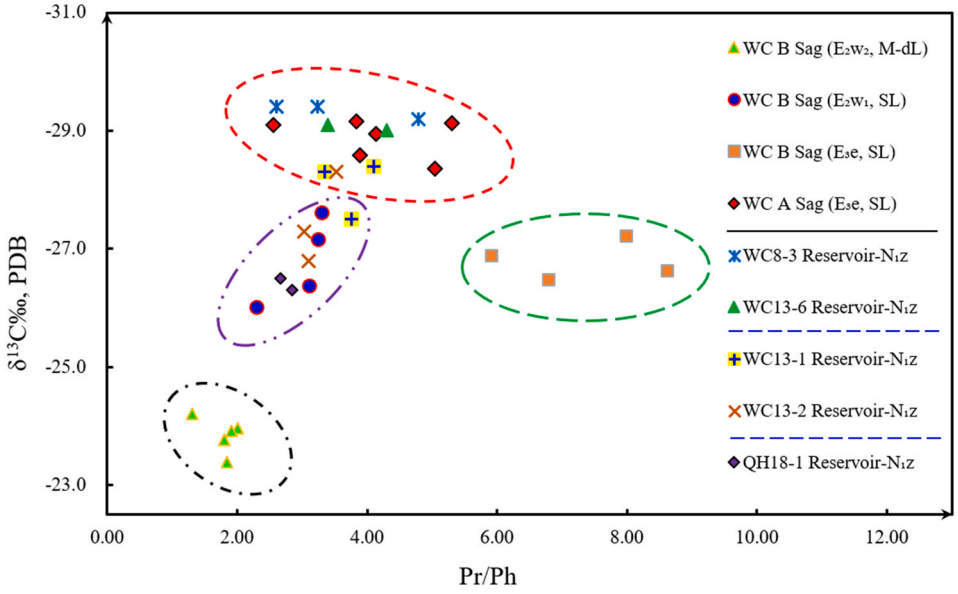

Fig. 5. Main geochemical parameter cross plot of the QH Uplift crude oil and the Wenchang Sag source rocks (WC A sag: Wenchang A sag; WC B sag: Wenchang B sag; N_1z: Zhujiang Formation; E_3e: Enping Formation; E_2w_1: Upper part of Wenchang Formation; E_2w_2: Middle part of Wenchang Formation; SL: Shallow Lacustrine; M-dL: Middle-deep Lacustrine).

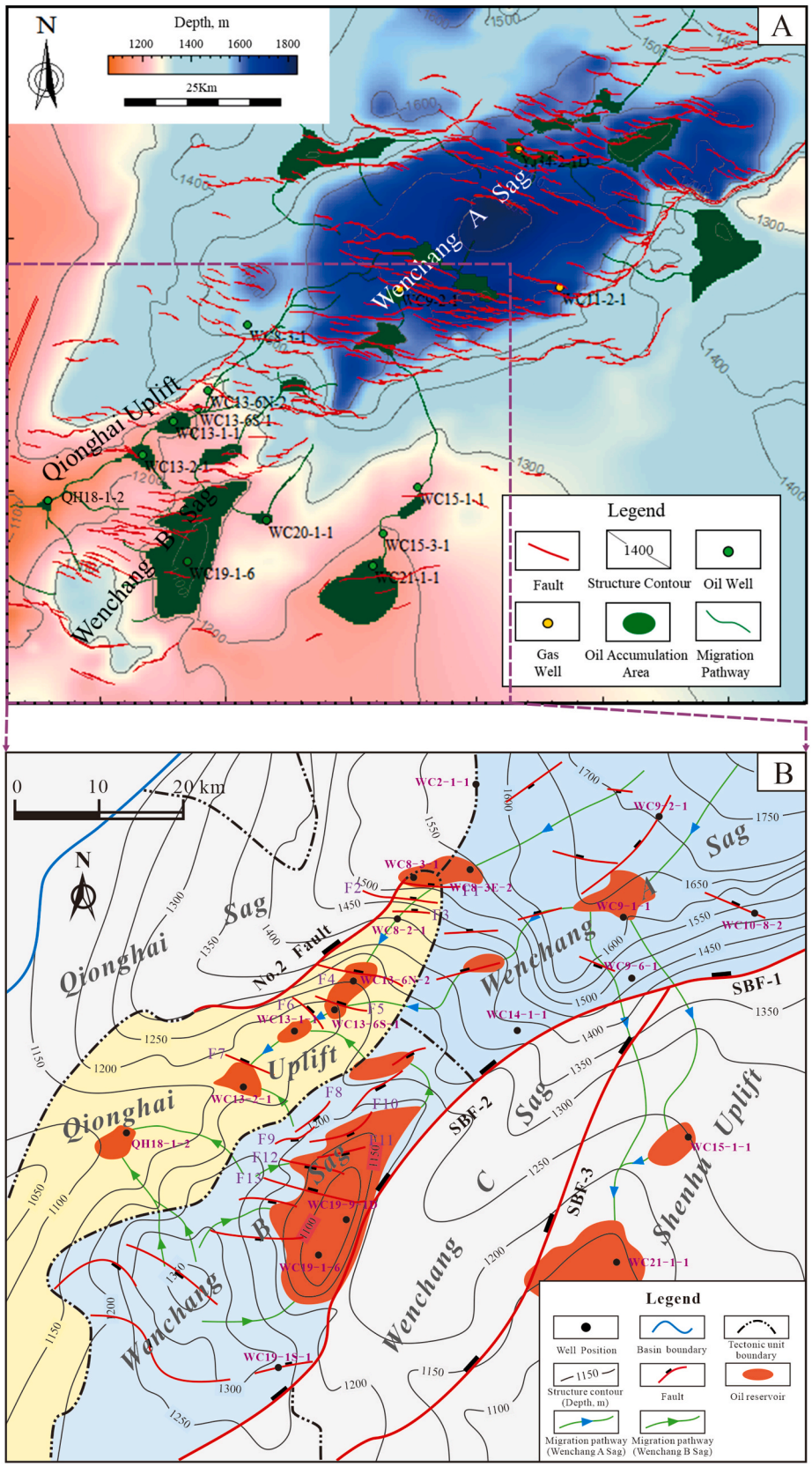

Fig. 6. Simulation of crude oil migration pathway and crude oil accumulation of the N_1z Formation under the control of the structure ridge.

Table 2
The main tracer parameters in the QH Uplift and the Wenchang Sag.

Area	Well Name	Crude oil density, g/cm^3	Ts/Tm	Total concentration of N-compounds, ng/mg
WC A Sag	WC8-3E-1	0.797	2.66	6.769
	WC9-1-1	0.761	2.51	5.805
	WC9-2-1	0.769	3.03	14.319
	WC9-6-1	0.752	2.36	3.739
	WC10-8-2	0.817	3.17	18.701
	WC14-3-1	0.781	2.25	13.109
WC B Sag	WC19-1-2	0.929	2.41	17.301
	WC19-1-6	0.861	2.38	15.432
East of QH Uplift	WC8-3-1	0.795	2.11	4.583
	WC13–6N-1	0.789	2.03	2.116
	WC13–6S-1	0.755	1.89	2.088
Middle of QH Uplift	WC13-1-2	0.805	2.05	8.472
	WC13-2-2	0.866	2.19	9.646
West of QH Uplift	QH18-1-2	0.919	2.56	10.105

(Xie et al., 2012) on source rocks of the Wenchang Sag showed that the E_3e Formation source rocks are mainly shallow lacustrine facies and the E_2w Formation source rocks are mainly medium-deep lacustrine facies, especially upper and middle parts of the E_2w Formation (E_2w_1 and E_2w_2). It is similar with the oil migration of near-source and far-source in the Zhu I Super-depression (Shi et al., 2020).

The E_3e Formation source rock is characterised by high-quality in the Wenchang A sag. The abundance of organic matter is high, with a TOC range of 0.42%–7.35% and an average TOC of 1.61%, the Wenchang A sag (TOC: total organic carbon). Additionally, the average vitrinite reflectance (R_o) of source rock is 0.99%, showing that source rock has basically reached mature stage, and its maximum can reach 1.63%. The analytical results showed kerogen type, the E_3e Formation source rock, is the II_2–III. Previous studies showed that the E_2w Formation source rock in the Wenchang A sag has entered over-mature stage and exhausted its generation potential before the time of traps formation, and thus, it basically has no effect on the formation of the reservoirs of the QH Uplift (Quan et al., 2015; Wang et al., 2016), which is consistent with the basin simulation result of Well WC11-2-1 (Fig. 3): the E_2w Formation source rock in the Wenchang A sag should not be taken into consideration.

The E_2w Formation source rock is superior in the Wenchang B sag. The range of TOC is between 0.42% and 7.81% and its mean is 3.14%, more than that of the E_3e Formation source rock in the Wenchang A sag. Additionally, the maximum of its R_o value can reach 1.12% and its mean is 0.85%, with I–II_1 type of kerogen, showing a mature stage characterised by generating oil.

The types of source rocks in the Wenchang Sag, only involving the Wenchang A sag and the Wenchang B sag, are complex, so we can find their differences in the distribution characteristics of biomarker compounds (Fig. 4 A and B). C_{30}-4-methyl sterane, which reflects the source of lower aquatic organisms, is enriched in the E_2w Formation source rocks, whereas its content is generally low in the E_3e Formation source rocks. However, the E_3e Formation source rocks are rich in resin compounds, such as 'W', 'T' and olivine, which are the biomarker compounds reflecting terrestrial high-grade plant sources. Tricyclic terpanes are commonly found in crude oil and source rock extracts, and it is often used as a reliable indicator of oil–source comparison and maturity (Chen and Liu et al., 2017). Under the normal circumstances, the higher

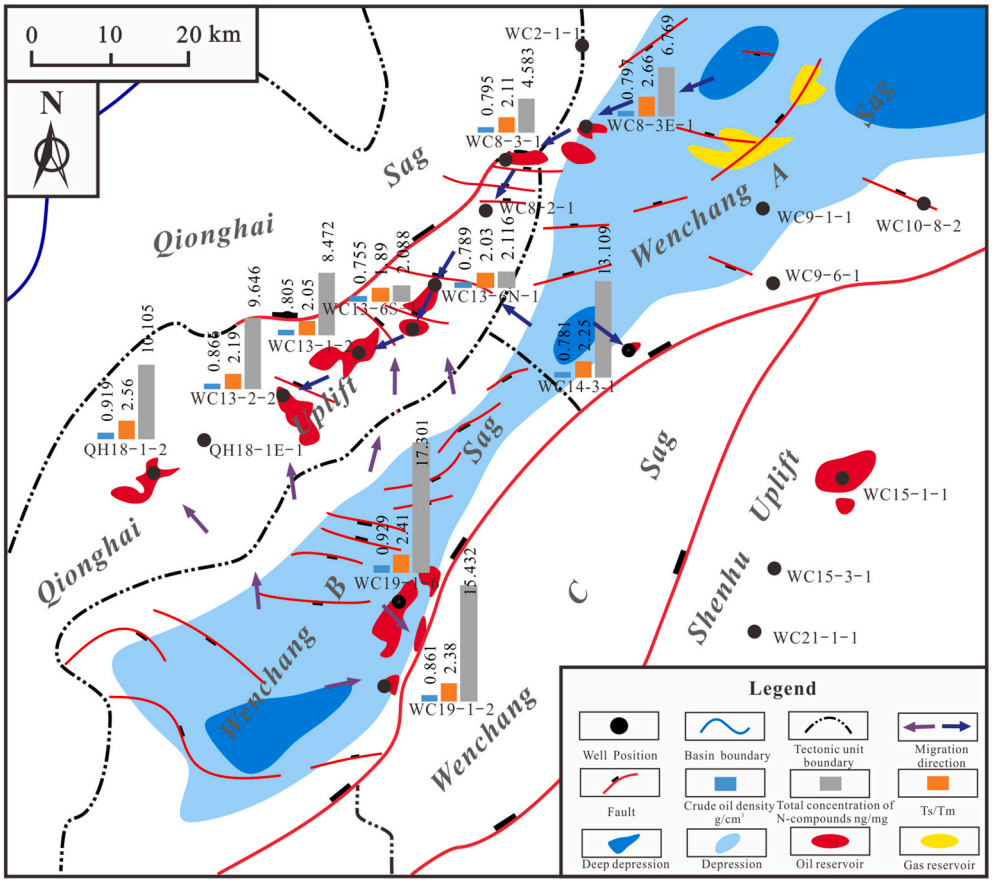

Fig. 7. Oil and gas reservoirs distribution on the plane and tracer parameters of crude oil migration pathways from the Wenchang sag to the QH Uplift. The tracer parameters include crude oil density, total concentration of nitrogen-containing compounds and Ts/Tm ratio, which represents the maturity of crude oil.

Table 3
QGF and QGF-E Results for typical wells in the QH Uplift.

Well Name	Depth (m)	Strata	QGF				QGF-E		Hydrocarbon Show
			Index (pc/pc)	Intensity (pc)	λ_{max} (nm)	$\triangle\lambda$ (nm)	I_{max} (pc)	λ_{max} (nm)	
WC13-1-1	1192	N_1z	8.13	12.3	438.1	145.0	86.5	372.0	Oil
WC13-1-1	1300	N_1z	4.00	4.9	432.1	152.2	24.5	363.0	Oil
WC13–6S-1	1095	N_1z	3.84	4.9	421.1	161.2	12.4	363.0	Dry
WC13–6S-1	1267	N_1z	6.84	11.2	433.3	142.2	94.1	374.0	Oil
WC8-2-1	1460	N_1z	4.52	6.4	439.1	156.8	25.7	362.0	Water
WC8-2-1	1742	N_1z	4.55	6.62	430.5	163.8	20.2	364.0	Water
WC8-3-1	1516	N_1z	4.67	6.7	417.1	164.4	43.1	377.0	Water
WC8-3-1	1870	N_1z	4.23	6.5	431.7	170.0	43.1	379.0	Water
WC8-3-1	2239	E_3z	3.66	4.8	431.3	153.4	13.8	359.0	Dry

Water: Oil-containing water layer.

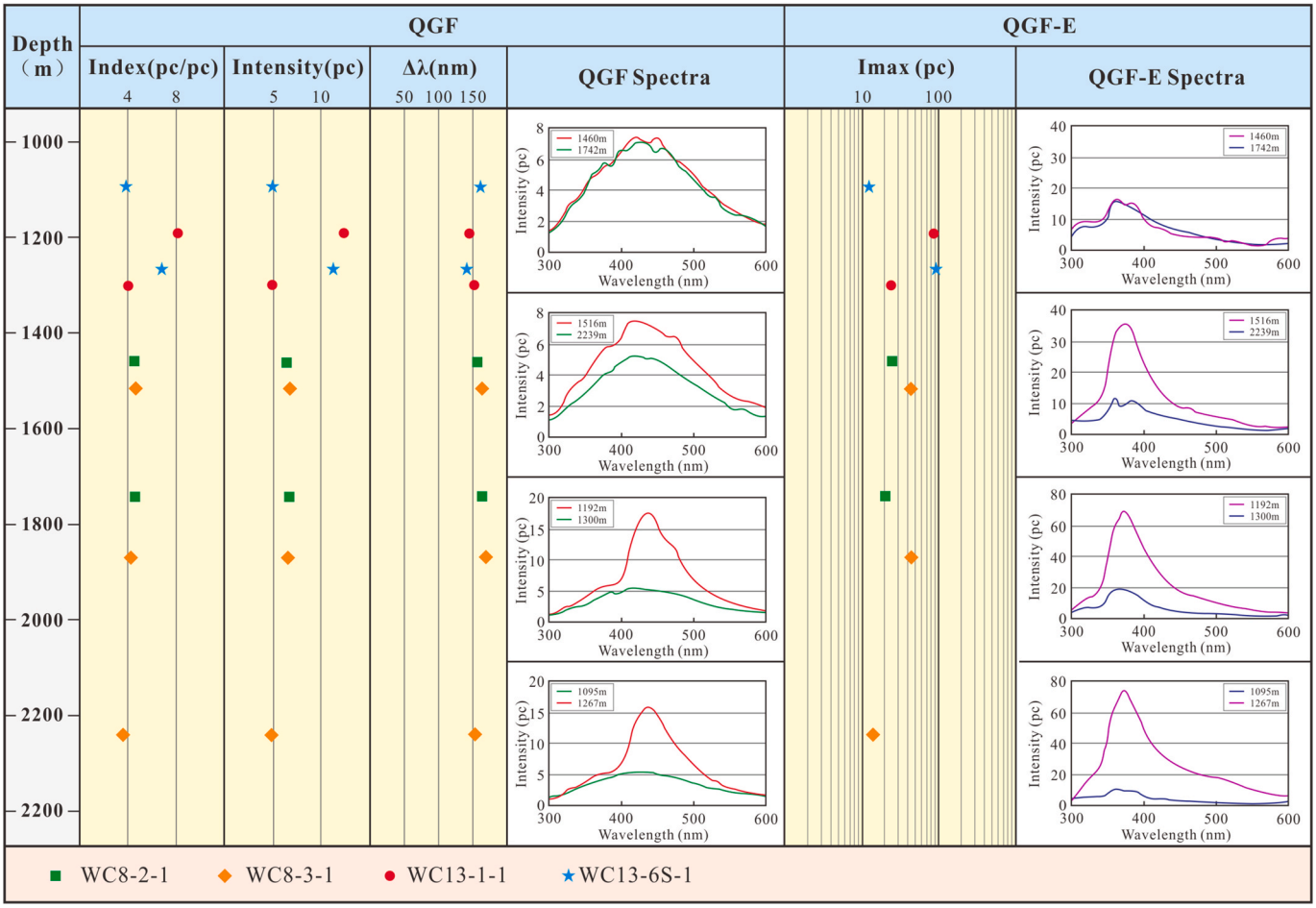

Fig. 8. The distribution characteristics of QGF and QGF-E parameters in the QH Uplift.

tricyclic terpane content, the higher organic matter maturity will be. The Wenchang A sag source rocks are rich in tricyclic terpane, and a 'declined' distribution is shown in the overall distribution. Content of C_{19}~C_{22} tricyclic terpanes is higher than C_{23}~C_{26} tricyclic terpane content. However, the tricyclic terpanes content in the source rocks of the Wenchang B sag is very low, and C_{19}~C_{22} tricyclic terpanes and C_{23}~C_{26} tricyclic terpanes show uniform potential distribution. In the similar condition, the Ts/Tm values of the source rocks in the Wenchang A sag are higher than those of the source rocks in the Wenchang B sag. Therefore, we conclude that the shallow lacustrine source rocks maturity in the Wenchang A sag is higher than that of the Wenchang B sag.

From the perspective of source rocks maturity, there are some differences between the Wenchang A sag and the Wenchang B sag. The E_3e Formation source rocks are only in mature stage and the E_2w Formation source rocks are in over-mature stage in the Wenchang A sag, but in the Wenchang B sag, the E_2w Formation source rocks just achieved the hydrocarbon generation threshold (Xu et al., 2000; Cheng et al., 2013), which also tell us that it is not necessary for this study to discuss the E_2w Formation source rocks of the Wenchang A sag and the E_3e Formation source rocks of the Wenchang B sag. Therefore, we mainly discuss the E_3e Formation source rocks of the Wenchang A sag and the E_2w Formation source rocks of the Wenchang B sag.

The crude oil geochemical characteristics in different locations of the QH Uplift are different (Fig. 4 D, E and F). In the eastern part of the QH Uplift, the content of resin compounds is slightly high, with a low content of C_{30}-4-methyl sterane. The C_{27}–C_{28}–C_{29} regular sterane content is high, and tricyclic terpanes are expressed as the main peaks of C_{19} and C_{20}. The C_{27}–C_{28}–C_{29} regular steranes are found in the anti- 'L' form in

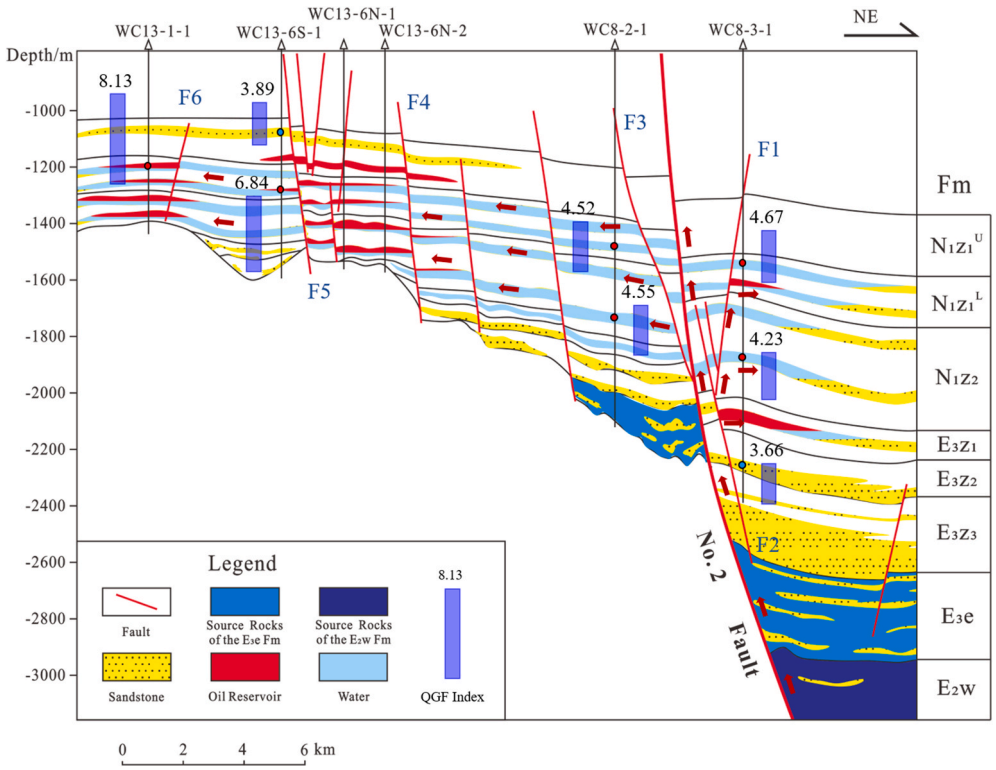

Fig. 9. QGF tracer profile of the Wenchang A sag and the QH Uplift, suggesting the direction of hydrocarbon migration from source rocks (E_3e and E_2w Formation) to reservoir (N_1z Formation). $N_1z_1^U$: Upper part of the N_1z_1 Formation; $N_1z_1^L$: Lower part of the N_1z_1 Formation.

the western part of the QH Uplift, with moderately low quantities of tricyclic terpanes. Moreover, the content of C_{19}–C_{22} tricyclic terpanes is equivalent to that of the C_{23}–C_{26} content. In the middle part of the QH Uplift, the characteristics of the C_{27}–C_{28}–C_{29} regular steranes are similar to those of the western part, the characteristics of tricyclic terpanes are also the same as above, but the maturity is higher, similar to the eastern part. However, oil origin can't be clearly judged by GC-MS analysis now, so it is very necessary for further study to obtain the geochemical parameters (Table 1), such as the carbon isotopes, pristane and phytane rations (Pr/Ph), and others.

Analysing the cross plot of the main geochemical parameters from crude oils and source rocks (Fig. 5), the E_3e Formation and E_2w_2 Formation source rocks in the Wenchang B sag have basically no effect on the crude oil accumulation of the QH Uplift. Although crude oils of the QH Uplift are mostly from source rocks of the E_3e Formation in the Wenchang A sag and the E_2w_1 Formation in the Wenchang A sag, shown in Fig. 5, the oil sources of three parts of the QH Uplift (i.e., east, middle and west) are different. The parameter values of crude oils in the eastern part of the QH Uplift (i.e., WC8-3 Reservoir and WC13-6 Reservoir) are close to those of the E_3e Formation source rocks in the Wenchang A sag, indicating crude oils, the eastern part, are supported by source rocks in the Wenchang A sag, and the E_2w_1 Formation source rocks in the Wenchang B sag only support crude oils for the western part (i.e., QH18-1 Reservoir). However, the crude oils of the central part, i.e., WC13-1 Reservoir and WC13-2 Reservoir, are from both the Wenchang A and B sags, indicating mixed sources.

4.2. Crude oils migration conduit

4.2.1. Structure ridge and significance for oil accumulation

The basin simulation software Trinity® was used to simulate the hydrocarbon migration pathway under the control of paleo-tectonic and hydrocarbon source kitchens for the N_1z oil reservoirs in the Uplift. The simulation results showed that the QH Uplift oil and gas originate from two main hydrocarbon-generating sags, the Wenchang A and B sags, through two different types of migration pathways (Fig. 6). Under the control of the structure ridge from the Wenchang Sag and the QH Uplift, the first style of migration pathway is the long-distance lateral migration from the north-eastern gentle-angle slope of the Wenchang A sag to the QH Uplift, which then forms oil reservoirs; and the second is the short-distance lateral migration from the south-eastern steep slope of the Wenchang B sag to the QH Uplift. From the top structure contour map, N_1z Formation (Fig. 6), the primary structure ridge of the QH Uplift tends to the northeast, so crude oil can be transported from the Wenchang A sag to the WC13-1 and WC13-2 Reservoirs rather than the QH 18-1 Reservoir of the QH Uplift. The secondary structure ridges of the QH Uplift are broom-shaped and converge to the Wenchang B sag, so crude oil can be transported from the Wenchang B sag to the QH18-1, WC13-2 and WC13-1 Reservoirs of the QH Uplift.

Although hydrocarbon migration was a complex process in which physical and chemical parameters change, all the tracer parameters changed regularly along the hydrocarbon migration pathway. Then, three parameters, namely, crude oil density, maturity (Ts/Tm) and total nitrogen-containing compound concentrations, were used to characterize the direction of crude oil migration (Table 2). For example, the crude oil density, which ranged from 0.789 to 0.919 g/cm^3, gradually increased from east to west in the QH Uplift. The Ts/Tm ratios and total nitrogen-containing compound concentrations also changed regularly, but there were the anomalous values in the local areas, especially the total nitrogen-containing compound concentration, because of the mixed sources.

The detailed data of crude oil density, maturity (Ts/Tm) and total nitrogen-containing compound concentration are shown in Fig. 7. From the eastern to the western parts of the QH Uplift, the density of crude oil, the total concentration of nitrogen-containing compounds and the Ts/Tm ratios gradually decrease and then increase. The density of crude oil and the total concentration of nitrogen-containing compounds in the Wenchang B sag are higher than those in the Wenchang A sag, and the

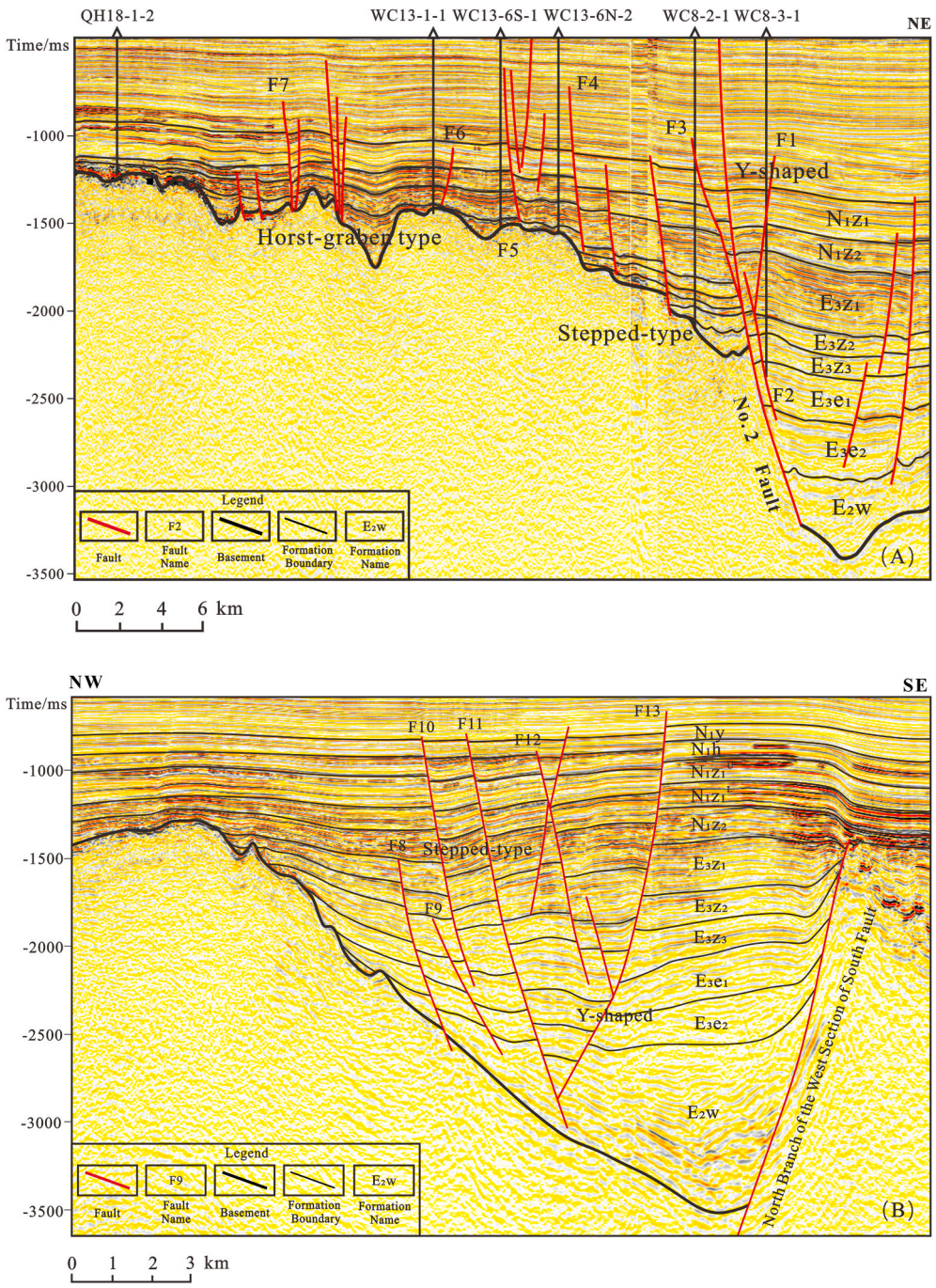

Fig. 10. The distribution characteristics of the fracture combination patterns on the profiles and the main secondary faults. (A): aa', Wenchang A sag and QH Uplift, F1–F7 are the main secondary faults; (B): bb', Wenchang B sag and QH Uplift, F8–F13 are the main secondary faults.

maturity of crude oil is slightly lower than that of the Wenchang A sag. The main source of heavy and highly mature crude oil in the western part of the QH Uplift is the Wenchang B sag; the light and highly mature crude oil in the eastern part is from the Wenchang A sag, indicating two migration pathways for crude oil in the QH Uplift. From the Wenchang A sag to the QH Uplift, crude oil is transported along a wide and gentle slope under the control of the structure ridge, whereas the crude oil from the Wenchang B sag migrates along the steep slope. The three parameters of the 13-6 Reservoir (i.e., WC13–6N-1 and WC13–6S-1), especially the total concentration of nitrogen-containing compounds, are obviously lower than those of other reservoirs. There are two factors resulting in the above phenomenon. One is that crude oils are only from the Wenchang A sag, which is different from the WC13-1, WC13-2 and QH18-1 Reservoirs, and the other is the hydrocarbon fractionation effect along the migration pathway. Combined with the simulation results of crude oil migration and the change of the above parameters, the real migration direction is shown in Fig. 7 and also prove the conclusion of oil–source correlation.

QGF and QGF-E analyses, reflecting the fluorescence features of oil inclusions within grains and residual hydrocarbons on grains surface, were used to identify hydrocarbon-bearing reservoirs, judge current or paleo-oil layers, analyse hydrocarbon properties, and trace hydrocarbon migration pathways amongst others (Bourdet et al., 2012; Liu and George et al., 2014). Some parameters, QGF Index, QGF Intensity, Lambda-Max (λ_{max}) and Delta Lambda ($\triangle\lambda$), were used to characterize the QGF results. The QGF-E results were characterised using the

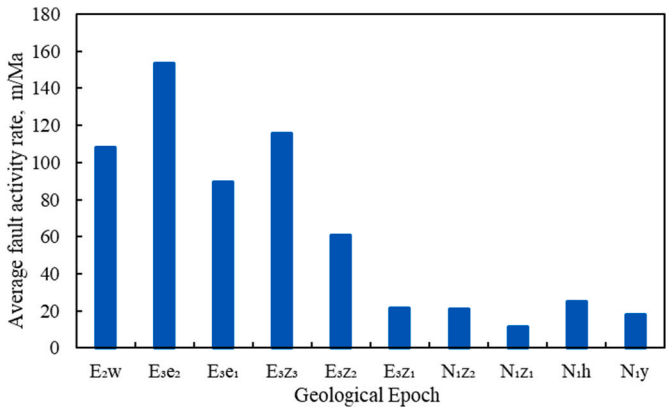

Fig. 11. The average fault activity rate curve of the ZF2 fault in the geologic epoch.

Maximum Intensity (I_{max}) and Lambda-Max (λ_{max}) parameters, as described by Liu et al. (2007). Previous studies have told us that QGF Index more than 4.0 indicates hydrocarbon migration occurring during the structure's geologic history (Liu et al., 2016). QGF and QGF-E analyses on the typical profile were also carried out to achieve some key parameters in the QH Uplift (Table 3). Taking the hydrocarbon shows into consideration, we found that the QGF Index was 4.0, and thus it was used as a criterion for judging the direction of crude oil migration from the Wenchang Sag to the QH Uplift (Fig. 8). Additionally, we believed that the sandstone may play an important role in crude oil migration pathway when the I_{max} value of QGF-E was generally greater than 20 pc. Therefore, the crude oil migration direction was determined by using QGF Index and QGF-E I_{max}.

The QGF tracer profile (Fig. 9) showed that the value of the QGF Index of the sand layer around the No. 2 Fault was over 4 and that it gradually increased from the bottom to the top, indicating that crude oil moved upward along No. 2 Fault from source rocks in the Wenchang A sag. Additionally, the QGF Index was between 3.66 and 8.13, the N_1z Formation in the QH Uplift. Thus, the sand bodies of the N_1z Formation

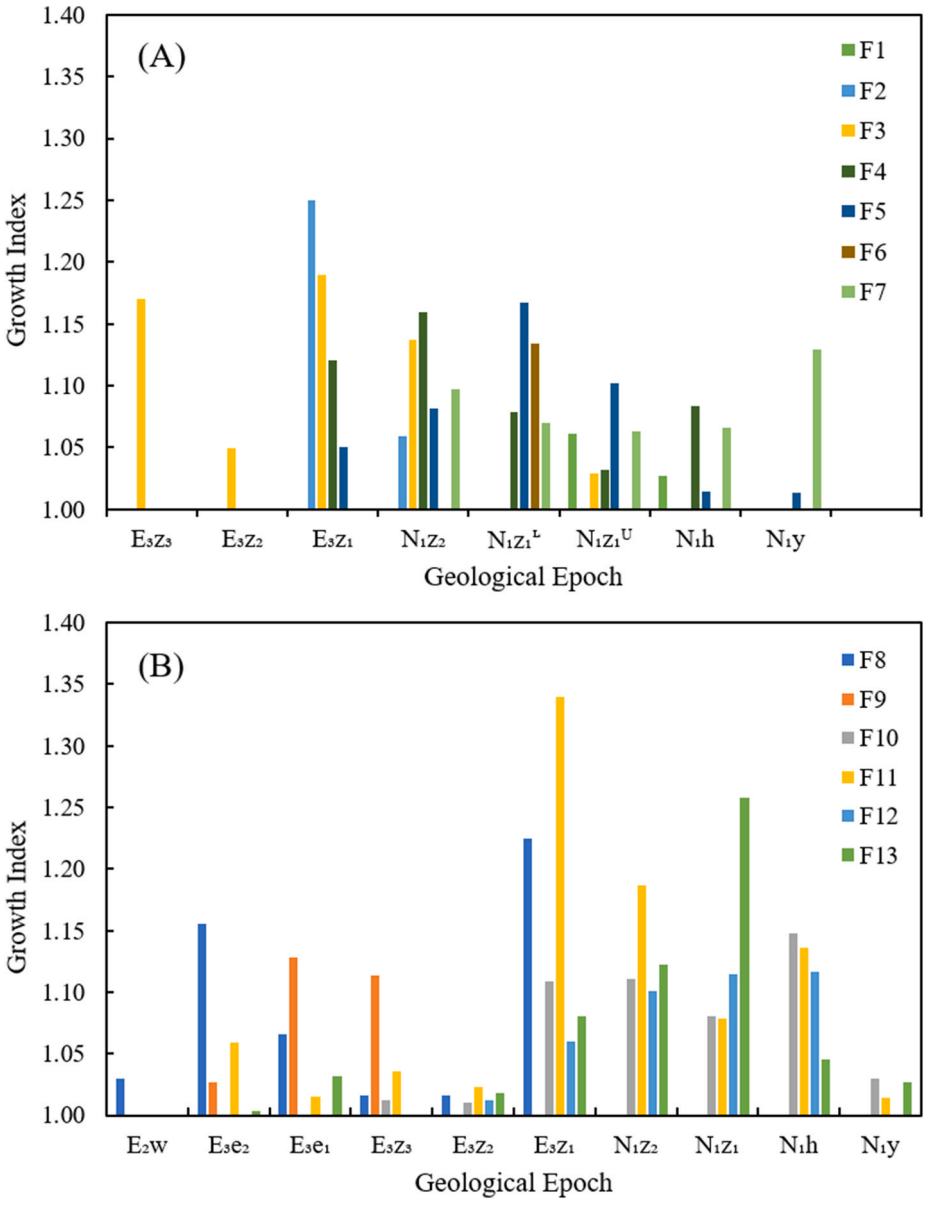

Fig. 12. The growth index histogram of the main secondary faults (F1–F13) at different geologic epochs. (A) The secondary faults distributed from the Wenchang A sag to the QH Uplift (F1–F7); (B) The secondary faults distributed from the Wenchang B sag to the QH Uplift (F8–F13).

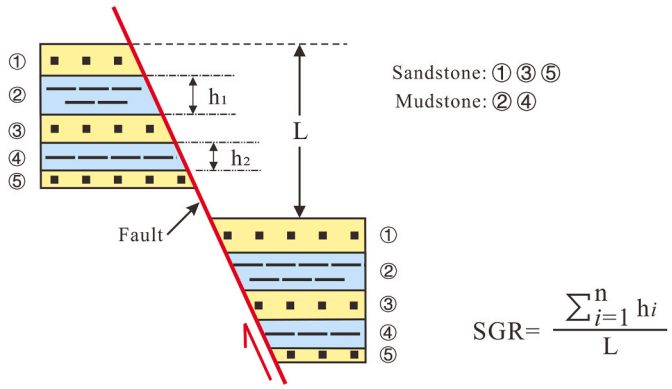

Fig. 13. Cartoon map showing mudstone smear quantitative calculation and the calculation formula (modified from Yielding et al., 1997). L is vertical fault distance and its unit is meter; h*i* is the *i*-th mudstone layer thickness broken by one fault and its unit is meter; n is the number of mudstone layers broken by one fault, dimensionless.

Table 4
Calculated SGR values of the Zhu III No. 2 Fault (ZF2) in the QH Uplift.

Well	WC13-2-1	WC13-1-1	WC13–6S-1	WC7-2-1	WC8-2-1	WC8-3-1
$N_1z_1^U$	0.55	0.32	0.36	0.64	0.88	0.83
$N_1z_1^L$	0.56	0.52	0.46	0.19	0.29	0.54
N_1z_2	0.57	0.27	0.53	0.45	0.36	0.19
E_1z_1	–	–	–	0.41	0.27	0.39
E_1z_2	–	–	–	0.26	0.22	0.16
E_1z_3	–	–	–	–	0.21	0.31

could be used as hydrocarbon migration conduits except for the $N_1z_1^U$ Formation. Therefore, crude oil migrated vertically along the No. 2 Fault; then crude oil would migrate laterally and accumulate along high-quality sand bodies forming the WC13-1, WC13-2 and QH18-1 Reservoirs under the control of the structure ridges.

Table 5
The NTG ratios of the N_1z and E_3z Formation in the Wenchang Sag and the QH Uplift.

Strata	Min (%)	Max (%)	Average (%)	Well Count
$N_1z_1^U$	0.7	68.4	22.7	46
$N_1z_1^L$	13.7	93.7	55.0	46
N_1z_2	10.7	92.6	60.5	43
E_3z_1	7.4	80.9	46.6	33
E_3z_2	25.8	77.4	54.3	30
E_3z_3	43.9	92.3	65.0	26

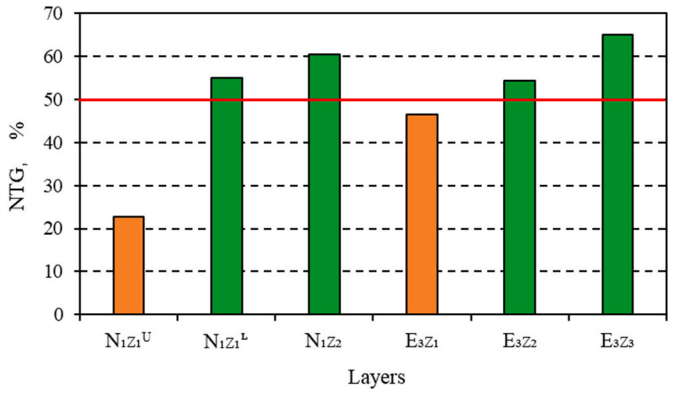

Fig. 15. The average NTG histogram of the N_1z and E_3z Formations. The lower limit of the NTG ratio is 50%, meaning that sand bodies are completely connected when the NTG ratio is more than 50%.

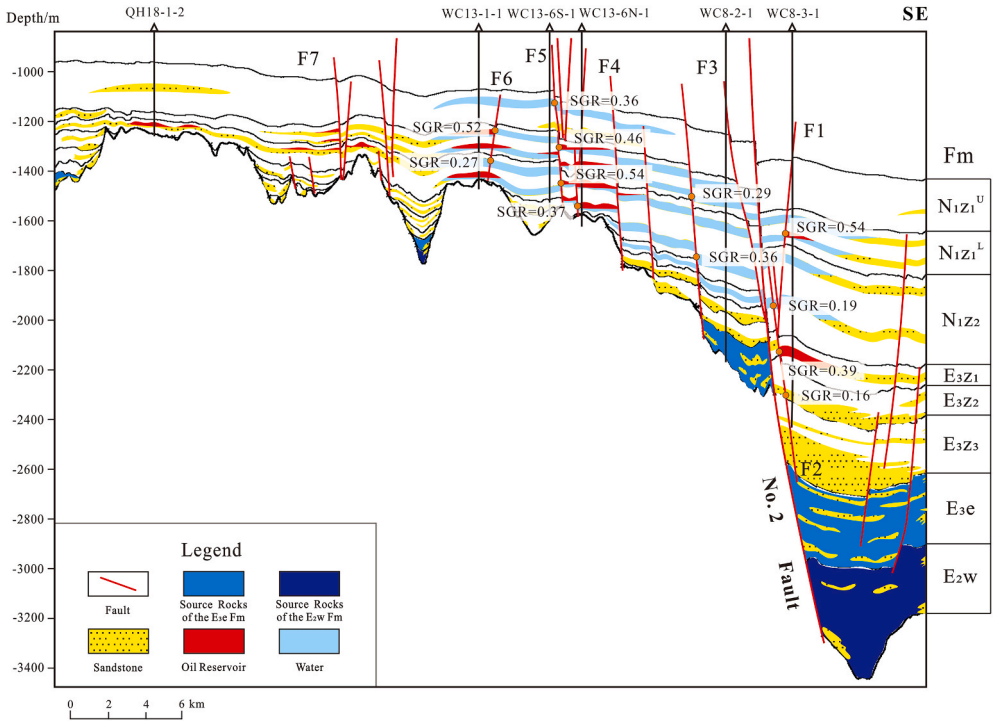

Fig. 14. The lateral closure evaluation of the main faults on the profile distributed from the Wenchang A sag to the QH Uplift (SGR) involving three reservoirs except WC13-2 and QH18-1.

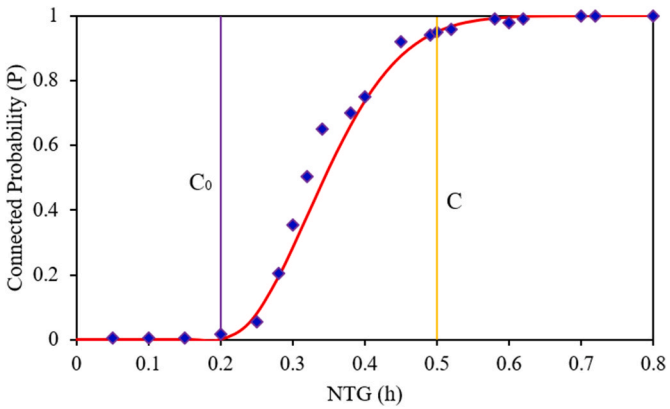

Fig. 16. The geometric connectivity assessing model of sand bodies in the carrier formation represented by the red curve, and the calibration of the relationship between the connected probability of sand bodies and the NTG ratio in the study area. When C was 0.5 ($P > 0.95$) and C_0 was 0.2, the mathematical model of sand body connectivity was consistent with the analysis of sand body connectivity in the Wenchang sag (A and B) and the QH Uplift. (For interpretation of the references to colour in this figure legend, the reader is referred to the Web version of this article.)

4.2.2. Fault activity and significance for oil accumulation

The development of the fault in the Zhu III Super-depression is very complicated, and faults have strong controlling effects on the migration and accumulation of crude oil (Chen et al., 2008). According to the development of the fault in the Zhu I Super-depression, the oil accumulation is divided into two types: favourable for shallow (N_1z and above) and deep (E_3e and E_2w) accumulations (Liu et al., 2017). Additionally, the fault combination pattern is a result of the complex tectonic stresses in the region. Different fault combination patterns have different geological significance for hydrocarbon accumulation (Fu et al., 2000; Nie and Jiang et al., 2011). Therefore, studying the impact of faults on hydrocarbon accumulation is inseparable from the study of the horizontal plane and the vertical section combinations of faults.

Extensional faults mainly developed in the Wenchang Sag, followed by localised torsional reverse faults due to stratigraphic reversing. These faults exhibit a variety of deformation patterns and combinations on the vertical section (Fig. 10). Single-fault patterns mainly include single-inclined, sloping-type, shovel-type, etc. The fault combination patterns mainly include Y-shaped, Horst–Graben type, stepped-type, etc. Among them, the combination of Y-shaped and stepped-type fractures account for the majority (Fig. 10 A and B).

The fault activity, which was divided into three stages, namely, the early extensional fault development period, the medium sliding extension fault development period, and the late strike–slip extension fault development period, played a vital role in effecting crude oil migration, accumulation and trap formation in this area (Fu et al., 2000; Cui et al., 2009; Li and Zhang et al., 2012; Zhang and Gan et al., 2013).

The early extensional fault development period, Late Cretaceous - Early Oligocene, was main source rock sedimentation period in the Wenchang Sag (Cui et al., 2009). The medium sliding extension fault development period, Late Oligocene - Early Miocene, was formation period of main traps in the Wenchang Sag and the QH Uplift (Gan and Zhang et al., 2009), i.e., the N_1z Formation and the E_3z Formation, thus providing a place for hydrocarbon generation and accumulation. The late strike–slip extension fault development period, middle Miocene - Holocene, was the regional cap rock deposition period (Ru, 1988). It efficiently transported oil and gas into the trap, forming the shallow anticline or stratigraphic lithologic oil reservoirs (Fu et al., 2000; Nie et al., 2011). For example, medium- or long-term inherited activity fault, like the Zhu III No. 2 Fault (abbreviated fault ZF2), is the main hydrocarbon migration pathway, which is beneficial to hydrocarbon migration from the Wenchang A and B sags to the QH Uplift.

The ZF2 fault (the hanging wall is the QH Sag and the footwall is the QH Uplift) is located at the QH Uplift, its northern end, and tends towards the northwest. The average fault activity rate initially increased and then decreased after 30 Ma (E_3z_3), but the rate finally stabilised (Fig. 10). The maximum value of the fault activity rate was 153.41 m/Ma and the minimum value was 11.41 m/Ma. The massive hydrocarbon generation time of source rocks in the Wenchang A sag, mainly the E_3e Formation, was early Miocene (Gan and Xie et al., 2014), and the hydrocarbon accumulation time was middle Miocene and beyond (Zhang et al., 2011a), which coincide with the fault activity period. Therefore, the ZF2 fault is a potential crude oil migration conduit.

The thickness of secondary faults measured from the seismic profiles (Fig. 10) is an important parameter for the growth index to evaluate the fault activity and to determine the fault activity period. Analysing the histogram of the fault growth index of the typical seismic profiles (Fig. 11), two important conclusions were reached: (1) The main active time of secondary faults in the Wenchang A sag close to the QH Uplift was from late Oligocene to middle Miocene (Fig. 12A), which is from the E_3z_3 Age to the N_1h Age. (2) The main active time of the secondary faults in the Wenchang B sag close to the QH Uplift was also from the end of late Oligocene to middle Miocene (Fig. 12B) but slightly later than the former. Combining the massive hydrocarbon generation time, the secondary faults could be excellent crude oil migration conduits.

Three main parameters could be used to quantitatively research the sealing ability of faults, namely, the shale smear factor (SSF: ratio of fault and mudstone thickness), clay smear potential (CSP: ratio of squared mudstone thickness and mudstone smearing distance) and the ratio of fault and mud (SGR: ratio of mudstone thickness and vertical fault) (Yielding, 1997; Cui et al., 2008; Wang et al., 2020). Considering the geologic factors of stratigraphic lithology and break distance, which have important computational significance for mudstone smearing, the SGR parameter was used to reflect the influence of the mudstone smear on the fault closure in this paper. The SGR parameter is the ratio of the mudstone thickness to the vertical fault distance of the faulted stratum. The mudstone thickness was obtained by analysing the natural potential curve of the well near the fault, and the vertical fault distance was measured by the seismic section.

The mudstone particles, immersed in the sandstone on the hanging wall and the footwall of fault, and sandstone physical properties are obviously reduced to have a high displacement pressure and lateral sealing effect on hydrocarbon. Yielding et al. (1997) proposed using the mudstone smear factor, SGR, to quantitatively evaluate the lateral sealing of faults (Fig. 13). The higher the content of fault shale, the better the fault closure will be.

Taking the ZF2 fault as an example, the SGR values were calculated by the above formula. The SGR values of six layers were between 0.19 and 0.88 (Table 4). The fault sealing of the N_1z Formation is better than that of the E_1z Formation. Considering the significance for crude oil migration and accumulation, we believe that crude oil will accumulate when SGR value is within a certain range. The E_1z_2 Formation acts as the hydrocarbon migration conduit when the SGR value is lower than the specific value. The upper part of the N_1z_1 Formation ($N_1z_1^U$) near the WC8-2-1 and WC8-3-1 wells acts as a seal when the SGR value reaches its high value of 0.83–0.88 and crude oils are also difficult to migrate laterally.

Through the calculation and statistical analysis of the SGR around the five wells (WC8-3-1, WC8-2-1, WC13–6N-1, WC13–6S-1 and WC13-1-1) on the key profile distributed from the Wenchang A sag to the QH Uplift (Fig. 14), combined with the hydrocarbon show and the distribution characteristics of oil reservoirs, the lower limit of the mudstone smear factor could be determined. The value of 0.37 could be the suitable key point of the SGR; when the in-situ value of SGR is higher than this value, the lateral sealing of the fault in the study area is better, which is conducive to the preservation of hydrocarbons. However, the fault closure is poor, and thus oil and gas cannot accumulate. However, this method has a drawback in that the profile without the well cannot

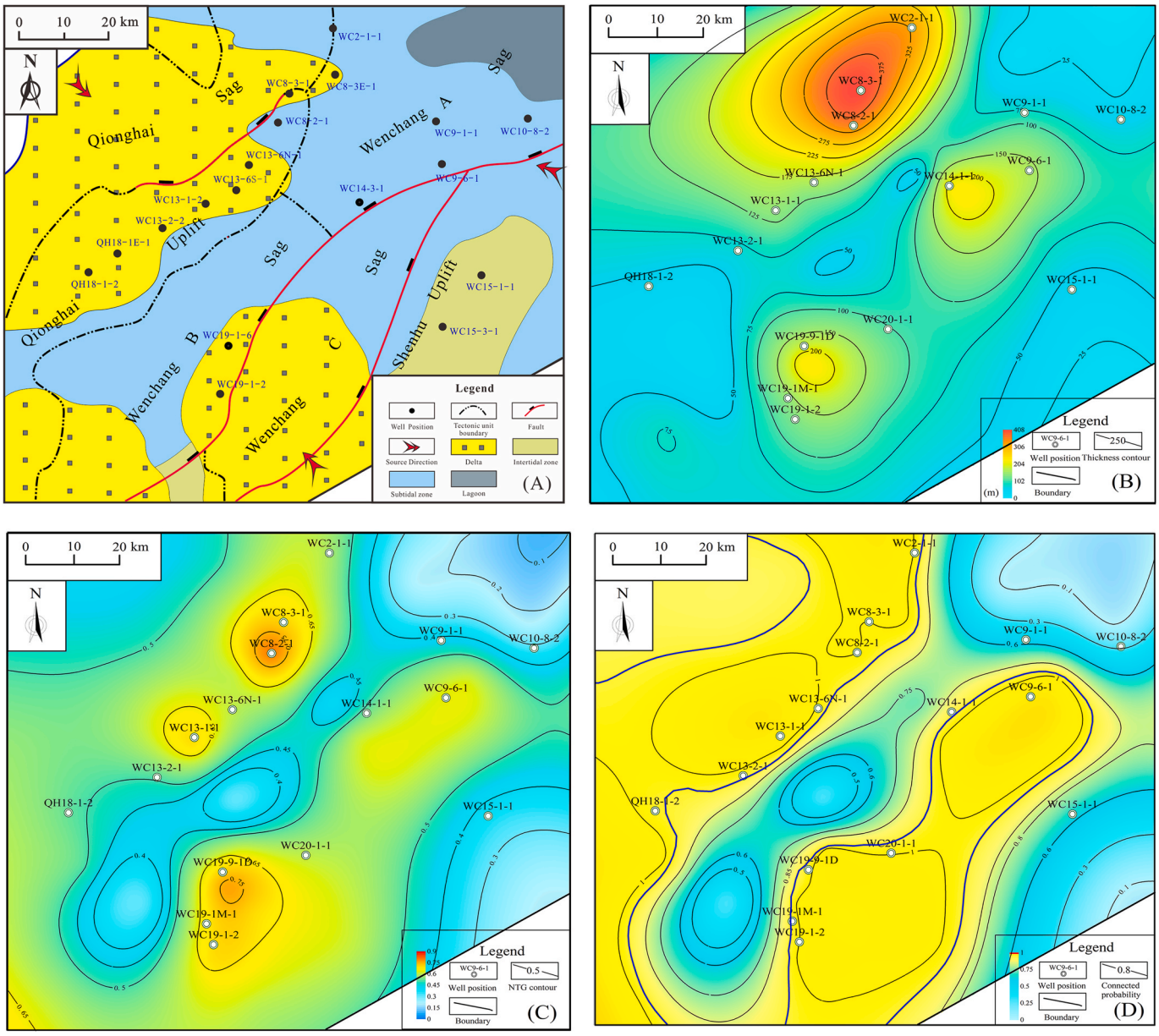

Fig. 17. The distribution characteristics of the connectivity of N_1z_2 sand bodies on the plane. (A) Sedimentary facies; (B) Sandstone thickness; (C) The NTG ratio distribution; (D) The connected probability of the N_1z_2 sand bodies. The sand bodies marked by blue solid lines are completely connected and the others are partially connected. (For interpretation of the references to colour in this figure legend, the reader is referred to the Web version of this article.)

be analysed this way. According to the seismic inversion profile, the qualitative analysis of the fault properties (such as tensional fault and so on) and the distribution of oil reservoirs, including hydrocarbon occurrences, the poor sealing ability of the faults is beneficial to hydrocarbon migration for the profile distributed from the Wenchang A sag, such as Fault F3 and Fault F4 in Fig. 14. On the contrary, Fault F1 and Fault F5 resulted in forming the WC8-3 and WC13-6 reservoirs respectively. Although faults act as crude oil migration conduits, the fault-sealing characteristics of the Wenchang B sag to the QH Uplift are different from those of the Wenchang A sag to the QH Uplift.

Based on the above results, the main faults in the Wenchang Sag could connect source rocks, including the E_3e Formation and the E_2w Formation, with shallow marine sandstones mainly involving in the E_3z Formation and the N_1z Formation. The transmission system is favourable for crude oil migration from the Wenchang Sag to the QH Uplift. The hydrocarbons generated in the Wenchang Sag migrate vertically along the fault under buoyancy conditions and then migrate along the structure ridge or sand body to the draped anticline of the QH Uplift and finally accumulate, especially forming the WC8-3 and WC13-6 Reservoirs.

4.2.3. *Sand body connectivity and significance for oil accumulation*

With the development of hydrocarbon exploration, research on transmission systems has gradually deepened. Hydrocarbon migration is not equivalent to migration throughout 3D space because it is restricted to certain paths for migration and accumulation (Bekele et al., 2002; Gibson et al., 2002). The sand body connectivity plays an important role in crude oil migration and accumulation, too (Ma and Zeng et al., 2012). Strengthening the research of sand body connectivity is of great significance for clarifying the configuration of transmission systems and for predicting migration path or conduit and accumulation position of crude oil.

In order to accurately describe the connectivity of sand bodies, many scholars have proposed the concept of sandstone percolation threshold

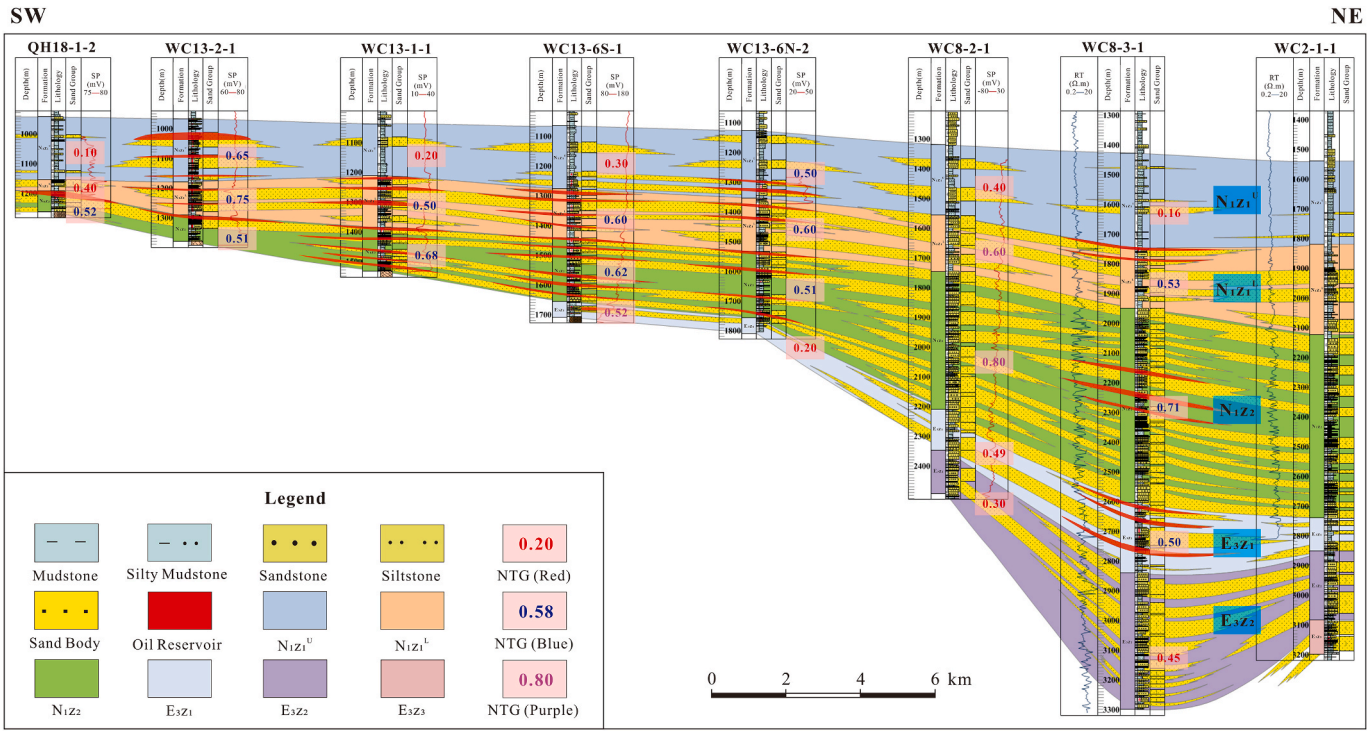

Fig. 18. The vertical distribution characteristics of the connectivity of sand bodies (represented by the NTG ratio) in the Wenchang A sag and the QH Uplift. Purple numbers indicate hydrocarbon shows, red numbers indicate dry layers and blue numbers indicate oil reservoirs. (For interpretation of the references to colour in this figure legend, the reader is referred to the Web version of this article.)

and complete connectivity coefficient. Allen (1978) considered that when the net-to-gross (NTG) ratio is greater than 50%, the sandstone is completely connected. King (1990) used percolation theory to determine the connectivity of two-dimensional and three-dimensional sand bodies, and the percolation thresholds are 0.688 and 0.276, respectively. Based on research of the characteristics of China's continental sedimentary basins, Qiu (1990) considered that when the NTG ratio is in the range of 30%–50%, sand bodies are semi-connected; when the NTG ratio is greater than 50%, they are completely connected. Luo et al. (2012) applied the method of reservoir description to construct the connecting probability formula of sand bodies and suggested that the critical value of the NTG ratio of the delta front sand bodies is 20% and that sand bodies are completely connected when the NTG ratio reaches 50%. Considering the characteristics of the study area and the above research, we adopted the connected probability of sand bodies to discuss the connectivity of sand bodies and their significance for hydrocarbon accumulation.

According to the lithological characteristics of 46 wells in the study area, the NTG ratio of the N_1z Formation ($N_1z_1^U$, $N_1z_1^L$ and N_1z_2) and the E_3z Formation (E_3z_1, E_3z_2 and E_3z_3) was calculated (Table 5). The calculation results showed that the NTG ratios of these six layers varied widely (Fig. 15). The average value of the upper part of the N_1z_1 Formation was 22.7%, whereas the values of the other layers (the E_3z Formation, the lower part of the N_1z_1 Formation and the N_1z_2 Formation) were between 46.6% and 65%. The NTG ratios of the N_1z_1 Formation were slightly lower, and the connectivity of the sand bodies was poor in the study area. The NTG ratios of the other layers were somewhat higher, so the sand bodies had good transport capacity for crude oil and provided a potential migration conduit for oil reservoirs in the QH Uplift.

According to the probability model which describes the spatial distribution of sand bodies, the relationship between the connected probability of sand bodies and the NTG ratio can be determined to describe the connectivity between sand bodies (King, 1990; Luo et al., 2012).

The formula is as follows:

$$P = \begin{cases} 0 & (h \le C_0) \\ 1 - e^{\left[-\frac{(h-C_0)^2}{b^2}\right]} & (h > C_0) \end{cases}$$

where P is the connected probability of sand bodies, h is the NTG ratio, C_0 is the percolation threshold, C is the completely connectivity coefficient and $b = (C–C_0)/\sqrt{3}$, which is the connectivity index.

According to the above analysis of crude oil migration and oil reservoirs distribution, we calculated the connected probability of sand bodies (P), determined by the NTG ratio, by using the above formula. The geometric connectivity assessing model of sand body connectivity was also established (Fig. 16). Therefore, we determined that C was 0.5 and C_0 was 0.2 in the study area.

Plane connectivity, sedimentary facies, the thickness of sandstone and the NTG ratio are important for analysing the connected probability of sand bodies. In this paper, taking the characteristics of the N_1z_2 Formation as an example, we found that the delta facies mainly developed at the edge of the Wenchang B sag and in the QH Uplift, whereas the subtidal zone mainly developed in the Wenchang A sag and the Wenchang B sag (Fig. 17A). According to the distribution of the sandstone thickness and the NTG ratio on the plane (Fig. 17 B and C), the sandstone thickness was generally more than 100 m, with this maximum value reaching 400 m in the east of the QH Uplift. The NTG ratio was generally more than 0.5 in the QH Uplift, and it varied slightly. The distribution of the connected probability of sand bodies was calculated, and the distribution area of the completely connected sand bodies is shown in Fig. 17D. Therefore, the sand bodies have strong connectivity on the plane in the QH Uplift. The completely connected sand bodies are beneficial to crude oils migration from the Wenchang sag to the QH Uplift.

The vertical connectivity of sand bodies refers to the ratio of number of sand bodies connected vertically to total number of sand layers (Zhang and Luo et al., 2011a; Ma, 2015). Based on the connectivity of

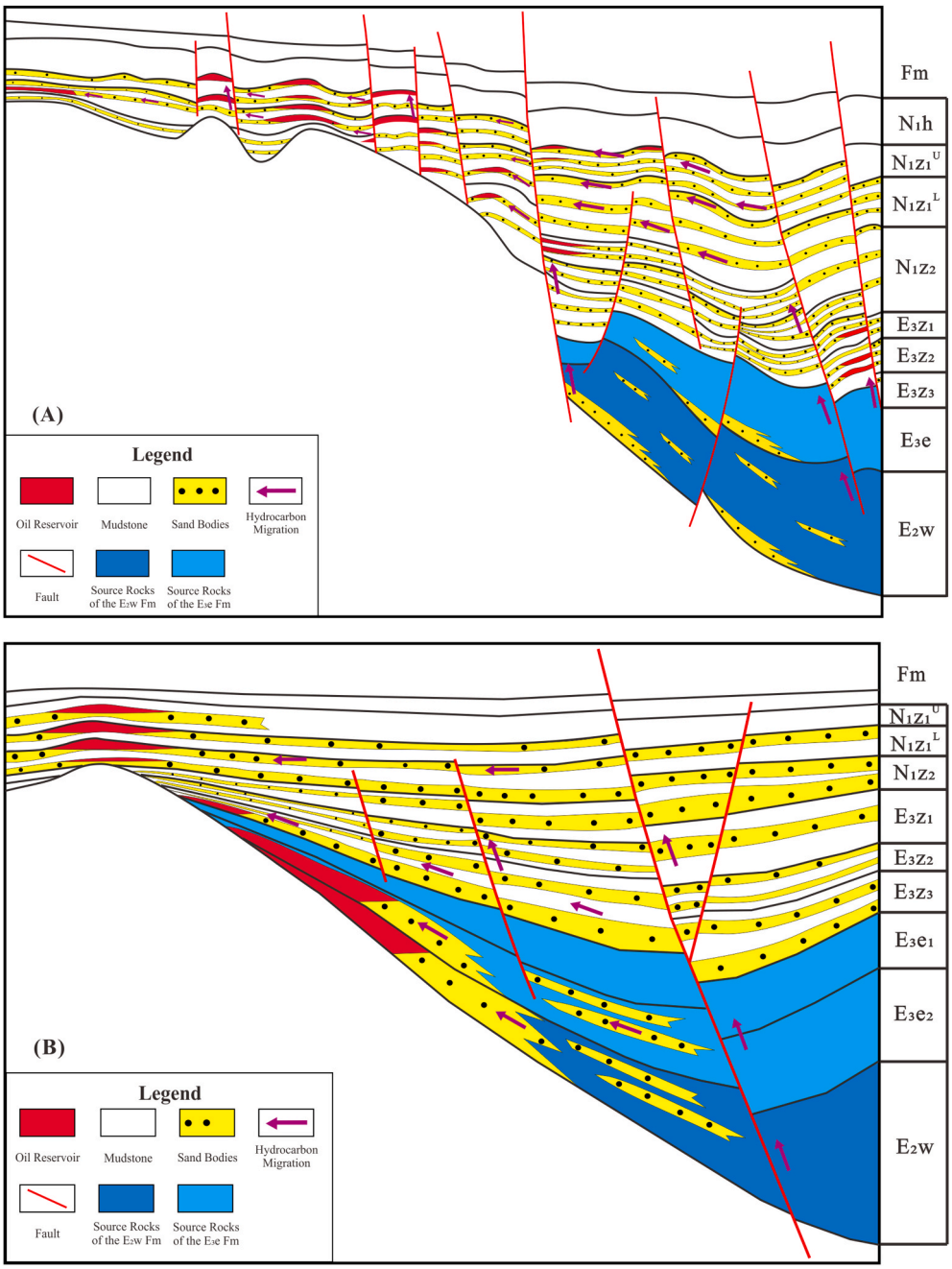

Fig. 19. The hydrocarbon migration and accumulation mode of the QH Uplift. (A) The hydrocarbon migrates from the Wenchang A sag to the QH Uplift; (B) The hydrocarbon migrates from the Wenchang B sag to the QH Uplift.

sand bodies on the plane and the lithologic distribution of the above five layers, the vertical distribution characteristics of sand bodies are shown in Fig. 18. Sand bodies of the N_1z Formation and E_3z Formation have good connectivity in the QH Uplift and are well lateral migration conduits for crude oils, especially the lower part of the N_1z Formation (N_1z_2). The NTG ratios of seven wells from left to right are 0.52, 0.51, 0.68, 0.62, 0.51, 0.80 and 0.71. Therefore, crude oils can migrate from the northeast to the southwest and accumulate in structural traps and lithological traps. Additionally, the hydrocarbon show is more active along the variation zone close to hydrocarbon migration pathways, where the connectivity of sand bodies obviously decreases and NTG ratio is less than 0.50, which is conducive to crude oil accumulation, so the lower part of the N_1z Formation is taken as an example, especially near WC8-2-1 and WC8-3-1. Because of the presence of the variation zone, hydrocarbons accumulated close Well WC8-3-1 instead of near Well WC8-2-1. Generally, the larger the NTG ratio, the more active the hydrocarbon show along the crude oil migration pathways in this study area.

4.3. Crude oils migration model

With the support of the qualitative and quantitative research of oil sources, crude oils migration pathways and transmission systems, the crude oils accumulation mode of the QH Uplift is summarized as the following two types, namely, the gentle-slope long-distance migration and accumulation mode, and the steep-slope short-distance migration and accumulation mode.

First, the gentle-slope long-distance migration and accumulation mode (Fig. 19A) is characterised by the composite transport of faults and sand bodies under the control of structure ridges. Because of the uniform

or uneven differential settlement of the basement, a flexible slope and sedimentary slope are formed. Firstly, crude oils are longitudinally displaced along stepped faults. Then, crude oils will migrate along sand bodies, gathering at the place where the connected probability of sand bodies decreases, for example, the sealing of fault, and at the low-magnitude folding structure. This model is fundamentally developed from the Wenchang A sag to the QH Uplift.

Second, the steep-slope short-distance migration and accumulation mode (Fig. 19B) is characterised by the composite transport of a Y-shaped fault and high-connectivity sand body. Because of the uneven settlement of the basement, the fault activity results in the formation of slope folding. The crude oils first move longitudinally along the Y-shaped fault. Then, they migrate laterally along the well-connected probability of sand bodies and accumulate in places where the structural reservoirs and stratigraphic-unconformity reservoirs are developed. This model is fundamentally developed from the Wenchang B sag to the QH Uplift.

5. Conclusion

Based on the above detailed research on the characteristics of the crude oil of five typical reservoirs in the QH Uplift and the source rocks in the Wenchang Sag, several conclusions were drawn as follows:

(1) The oil–source correlation analysis reveals that the origins of crude oils are complex, characterised by a single oil source on both sides of the QH Uplift and a mixed source in the central part. Crude oils of the eastern, the QH Uplift, are from the Wenchang A sag, and crude oils of western part are from the Wenchang B sag, whereas the oil sources of the central part are the Wenchang A and B sags.
(2) Structure ridges, faults and sand bodies constitute a complex hydrocarbon transmission system from the Wenchang Sag to the QH Uplift. Under the control of structure ridges, crude oils first migrate along the well-connected sand bodies and the open faults. Crude oils accumulate at a low-magnitude folding structure in the western and central parts of the QH Uplift, and gather at the sealed faults in the eastern part.
(3) Two types of crude oil migration and accumulation modes are summarized for oil reservoirs of the QH Uplift. The gentle-slope long-distance migration and accumulation mode is fundamentally developed from the Wenchang A sag to the QH Uplift. Whereas the steep-slope short-distance migration and accumulation mode is fundamentally developed from the Wenchang B sag to the QH Uplift.

Declaration of competing interest

The authors declare that they have no known competing financial interests or personal relationships that could have appeared to influence the work reported in this paper.

Acknowledgments

This study was successfully accomplished, with the support of the National Science and Technology Major Project (Grant No. 2016ZX05006-003). We gratefully acknowledge the Zhanjiang Branch of China National Offshore Oil Corporation for providing geochemical data of rock samples and seismic data.

Appendix A. Supplementary data

Supplementary data to this article can be found online at https://doi.org/10.1016/j.petrol.2021.108943.

Credit author statement

Guangjie Xie: Formal analysis, Investigation, Writing – original draft preparation, Supervision; Dongxia Chen: Conceptualization, Resources, Writing- Reviewing and Editing; Lu Chang: Methodology, Software; Jinheng Li: Data curation; Zhijun Yin: Validation.

References

Allen, J.R.L., 1978. Studies in fluviatile sedimentation: an exploratory quantitative model for the architecture of avulsion-controlled alluvial suites. Sediment. Geol. 21 (2), 129–147.
Bekele, E., Person, M.A., Rostron, B.J., Barnes, R., 2002. Modelling secondary oil migration with core-scale data: viking Formation, Alberta basin. AAPG (Am. Assoc. Pet. Geol.) Bull. 86 (1), 55–74.
Bourdet, J., Eadington, P., Volk, H., George, S.C., Pironon, J., Kempton, R., 2012. Chemical changes of fluid inclusion oil trapped during the evolution of an oil reservoir: jabiru-1A case study (Timor Sea, Australia). Mar. Petrol. Geol. 36 (1), 118–139.
Chen, J., Xu, G.Q., 2008. Type and Distribution Characteristics of the Faults in the B Depression of the Zhujiangkou Basin, China, vol. 3. Journal of Chengdu University of Technology (Science & Technology Edition, pp. 309–316.
Chen, Z.L., Liu, G.D., Wei, Y.Z., Gao, G., Ren, J.L., Yang, F., Ma, W.Y., 2017. Distribution pattern of tricyclic terpanes and its influencing factors in the Permian source rocks from Mahu Depression in the Junggar Basin. Oil Gas Geol. 38 (2), 311–322.
Cheng, P., 2013. Research on the Source and Formation of Oil Pools in the Western Pearl River Mouth Basin. University of Chinese Academy of Science.
Cheng, P., Xiao, X.M., Tian, H., Huang, B.J., Wilkins, R.W.T., Zhang, Y.Z., 2013. Source controls on geochemical characteristics of crude oils from the Qionghai uplift in the western Pearl River Mouth Basin, offshore south China Sea. Mar. Petrol. Geol. 40, 85–98.
Cui, S.S., He, J.X., Chen, S.H., Zou, H.P., Cui, J., 2009. Development characteristics of Pearl River Mouth Basin and its geological conditions for oil and gas accumulation. Natural Gas Geoscience 20 (3), 384–391.
Cui, Y.M., Lu, Z.Y., Zhong, W., 2008. Study on fault sealing in fang 169 block of zhaozhou oilfield. Lithologic Reservoirs 20 (3), 83–88.
Fu, L.X., Wang, D.L., Xiao, Y.Y., 2000. Effect of tensional faulting on secondary migration of hydrocarbon. Journal of China University of Petroleum (Edition of Natural Science) 4, 71–74, 128-129.
Fu, N., Li, Y.C., Sun, J.X., Xu, J.Y., 2011. Recognition of oil source and source rocks in Zhu III depression. Earth Sci. 25, 1121–1130.
Gan, J., Xie, Y.H., Zhang, Y.C., Li, X.S., Huang, B.J., Li, H., Liu, K., Wu, Y.Y., You, L., 2014a. A relationship between abnormally high pressure in Enping Formation and hydrocarbon accumulation in Wenchang A sag. China Offshore Oil Gas 26 (6), 7–13.
Gan, J., Zhang, Y.C., Deng, Y., Wang, Z.F., Li, X.S., Lu, J., Yang, J.H., Zheng, R.F., 2009. Main controls over Paleogene natural gas accumulation and its exploration direction in Wenchang A sag, the western Pearl River Mouth basin. China Offshore Oil Gas 21 (6), 367–371.
Gan, J., Zhang, Y.C., Deng, G.J., Lu, J., Zheng, R.F., 2014b. Forming conditions and hydrocarbon accumulation patterns of the Neogene low resistivity reservoirs in low-amplitude structure of Qionghai Salient. Oil Gas Geol. 35 (3), 311–316+349.
Gibson, R.G., Dzou, L., 2002. Petroleum Migration Pattern in Faulted Traps Deduced from Geochemical and Fault-Seal Studies, Columbus Basin, Offshore Trinidad. AAPG Annual Meeting, Houston, Texas.
Gong, Z.S., Li, S.T., 2004. Dynamic Research of Oil and Gas Accumulation in Northern Marginal Basins of South China Sea. Science Press, Beijing.
He, J.X., Liu, H.L., Yao, Y.J., Zhang, S.L., Luan, X.W., 2008. Petroleum and Gas Geology and Resources Prospects in Northern Marginal Basins of South China Sea. Petroleum Industry Press, Beijing.
He, M., Graham, S., Scheirer, A.H., Peters, K.E., 2014. A basin modelling and organic geochemistry study of the Vallecitos syncline, San Joaquin Basin, California. Mar. Petrol. Geol. 49, 15–34.
Jiang, H., Wang, H., Li, J.L., Chen, S.P., Lin, Z.L., Fang, X.X., Cai, J., 2009. Research on hydrocarbon pooling and distribution patterns in the zhu-3 depression, the Pearl River Mouth Basin. Oil Gas Geol. 30 (3), 275–281+286.
Jiang, H., Wang, H., Xiao, J., Lin, Z.L., Lü, X.J., Cai, J., 2008. Tectonic inversion and its relationship with hydrocarbon accumulation in zhu-3 depression of Pearl River Mouth Basin. Acta Pet. Sin. 3, 372–377.
Jiang, W.R., Zhou, W.W., 1998. Hydrocarbon accumulation and diagenesis of the zhu III depression. Acta Pet. Sin. 4, 91–97.
King, P.R., 1990. The Connectivity and Conductivity of Overlapping Sand Bodies.
Li, C.R., Zhang, G.C., Liang, J.S., 2012. Characteristics of fault structure and its control on hydrocarbons in the Beibuwan Basin. Acta Pet. Sin. 33 (2), 195–203.
Li, H., Chen, S.H., Zhang, Y.C., Niu, C.Y., Zhang, K.K., Ye, Q., Hu, G.W., 2014. Faults in the zhu-3 depression of Pearl River Mouth Basin and their control over hydrocarbon accumulation. Mar. Geol. Quat. Geol. 34 (3), 115–124.
Li, H., Zhang, Y.C., Niu, C.Y., Lu, J., Zhou, G., Zhan, Z.P., 2015. Hydrocarbon accumulation pattern of Wenchang B sag, western Pearl River Mouth Basin in the northern South China Sea. Mar. Geol. Quat. Geol. 35 (4), 133–140.
Li, J.H., Chen, D.X., Chang, L., Xie, G.J., Shi, X.B., Wang, F.W., Liao, W.H., Wang, Z.Y., 2020. Quality, Hydrocarbon Generation, and Expulsion of the Eocene Enping Formation Source Rocks in the Wenchang Depression, Western Pearl River Mouth Basin, South China Sea. Energy Exploration & Exploitation.

Li, J.L., Wang, H.R., Zhang, J.X., Li, Q., Liu, H., 2010. Distribution, geometry and hydrodynamic mechanism of tidal sand ridges in the Zhujiang Formation, the western Zhujiangkou Basin. Oil Gas Geol. 31 (5), 671–677.
Li, J.L., Lei, B.H., Zheng, Q.G., Duan, L., Yan, Y., 2015. Stress field evolution and its controls on oil accumulation in the Wenchang sag. Geotect. Metallogenia 39 (4), 601–609.
Li, S.M., Pang, X.Q., Zhang, B.S., Xiao, Z.Y., Gu, Q.Y., 2010. Oil-source rock correlation and quantitative assessment of Ordovician mixed oils in the Tazhong Uplift, Tarim Basin. Petrol. Sci. 7 (2), 179–191.
Li, Z., Li, L., Xing, L., Liu, Y., Zhang, M., Wang, X., Cao, C., Wang, Z., 2018. Development of new method for D/H ratio measurements for volatile hydrocarbons of crude oils using solid phase micro-extraction (SPME) coupled to gas chromatography isotope ratio mass spectrometry (GC-IRMS). Mar. Petrol. Geol. 89 (12), 232–241.
Liu, K.Y., Eadington, P., Middleton, H., Fenton, S., Cable, T., 2007. Applying quantitative fluorescence techniques to investigate petroleum charge history of sedimentary basins in Australia and Papuan New Guinea. J. Petrol. Sci. Eng. 57, 139–151.
Liu, K.Y., George, S.C., Lu, X.S., Gong, S., Tian, H., Gui, L., 2014. Innovative fluorescence spectroscopic techniques for rapidly characterising oil inclusions. Org. Geochem. 72, 34–45.
Liu, K.Y., Lu, X.S., Gui, L.L., Fan, J.J., Gong, Y.J., Li, X.L., 2016. Quantitative fluorescence techniques and their applications in hydrocarbon accumulation studies. Earth Sci. 41 (3), 373–384.
Liu, Z.F., Wu, K.Q., Ke, L., Wang, S.L., Yu, K.P., Zhu, W.Q., 2017. Main factors controlling hydrocarbon accumulation in northern sub-sag belt of the Zhu-1 Depression, Pearl River Mouth Basin. Oil Gas Geol. 38 (3), 561–569.
Luo, X.R., Lei, Y.H., Zhang, L.K., Chen, K.Y., Chen, Z.K., Xu, J.H., Zhao, J., 2012. Characterization of carrier formation for hydrocarbon migration: concepts and approaches. Acta Pet. Sin. 33 (3), 428–436.
Ma, Q., 2015. Quantitative Research of the Conducting Performance of Dense Sandstone Transportation Systems—With Chang 8 Reservoir of HH Oilfield in Ordos Basin for Example. Xi'an Shiyou University.
Ma, Z.L., Zeng, J.H., Zheng, L.J., 2012. Hydrocarbon migration pathway in carrier layer junction based on steady filling. Petroleum Geology & Experiment 34 (1), 89–93+98.
Nie, F.J., Jiang, M.Z., Li, S.T., 2011. Petroleum migration system in zhu III depression, Pearl River Mouth Basin, China south Sea. Petroleum Geology & Experiment 33 (4), 392–401.
Pepper, A.S., Corvi, P.J., 1995. Simple kinetic models of petroleum formation. Part I: oil and gas generation from kerogen. Mar. Petrol. Geol. 12 (3), 291–319.
Piero, E., Hensen, C., Haeckel, M., Rottke, W., Fuchs, T., Wallmann, K., 2016. 3-D numerical modelling of methane hydrate accumulations using PetroMod. Mar. Petrol. Geol. 71, 288–295.
Qiu, Y.N., 1990. Sedimentology workflow of reservoir. Petrol. Explor. Dev. 1, 85–90.
Quan, Y., Liu, J., Hao, F., Zhao, D., Wang, Z., Tian, J., 2015. The origin and distribution of crude oil in zhu III sub-basin, pearl river mouth basin, China. Mar. Petrol. Geol. 732–747.
Quan, Y., Hao, F., Liu, J., Zhao, D., Tian, J., Wang, Z., 2017. Source rock deposition controlled by tectonic subsidence and climate in the western Pearl River Mouth Basin, China: evidence from organic and inorganic geochemistry. Mar. Petrol. Geol. 79, 1–17.
Ru, K., 1988. Development and its tectonic significance of superimposed basins in the northern margin of the south China Sea. Oil Gas Geol. 1, 22–31.
Shi, H.S., Dai, Y.D., Liu, L.H., Jiang, H., Li, H.B., Bai, J., 2015. Geological characteristics and distribution model of oil and gas reservoirs in zhu I depression, Pearl River Mouth Basin. Acta Pet. Sin. 36 (S2), 120–133+155.
Shi, Y.L., Zhang, X.T., Zhu, J.Z., Long, Z.L., Jia, Z.Y., Zhang, X.L., 2020. Statistics on the main geological factors controlling hydrocarbon accumulation of near and distal sources in Zhu I depression and the physical simulation experiment of hydrocarbons migration. China Offshore Oil Gas 32 (5), 26–35.
Sun, Q.S., Xiao, F., Gao, X.Y., Zong, W.M., Li, Y.F., Zhang, J., Sun, S.L., Chen, S.W., 2019. A new discovery of Mesoproterozoic erathem oil, and oil–source correlation in the Niuyingzi area of western Liaoning Province, NE China. Mar. Petrol. Geol. 110, 606–620.
Wang, C., Zeng, J.H., Lin, X.Y., Liu, X.F., Wang, F.F., Zhang, J.Y., Jia, K.Y., 2017. Utility of GOI, QGF, and QGF-E for interpreting reservoir geohistory and oil remigration in the Hudson oilfield, Tarim basin, northwest China. Mar. Petrol. Geol. 86.
Wang, K., Zhang, Y., Huang, S.B., Chen, J.Y., 2016. Characteristics and thermal evolution history of source rocks in the wenchang-A sag, Pearl River basin. Geol. Resour. 25 (2), 196–203.
Wang, W.Y., Pang, X.Q., Chen, Z.X., Chen, D.X., Ma, X.H., Zhu, W.P., Zheng, T.Y., Wu, K. L., Zhang, K., Ma, K.Y., 2020. Improved methods for determining effective sandstone reservoirs and evaluating hydrocarbon enrichment in petroliferous basins. Appl. Energy 261, 114457.
Wang, Y., Liu, L.F., Ji, H.C., Song, G.J., Luo, Z.H., Li, X.Z., Xu, T., Li, L.Z., 2018. Origin and accumulation of crude oils in Triassic reservoirs of Wuerhe-Fengnan area (WFA) in Junggar Basin, NW China: constraints from molecular and isotopic geochemistry and fluid inclusion analysis. Mar. Petrol. Geol. 96.
Xie, R.Y., Huang, B.J., You, J.J., 2012. The Geochemical characteristics and hydrocarbon generation potential of high-quality source rock in Wenchang sag. China Mining Magazine 21 (9), 69–71+75.
Xie, Y.H., 2011. Discovery on neocene marine low resistivity-light oilfields in the western of the Pearl River Mouth Basin. Eng. Sci. 13 (5), 16–22.
Xu, S.H., Zhu, Y.Q., 2010. Well logs response and prediction model of organic carbon content in source rocks—a case study from the source rock of Wenchang Formation in the Pearl River Mouth Basin. Petroleum Geology & Experiment 32 (3), 290–295, 300.
Xu, X.D., Huang, B.J., Li, L., Zhang, M.Q., 2000. A study on the migration and accumulation of oil and gas in Qionghai uplift Zhu III depression. Petrol. Explor. Dev. 27, 41–44.
Yielding, G., Freeman, B., Needham, D.T., 1997. Quantitative fault seal prediction. AAPG (Am. Assoc. Pet. Geol.) Bull. 81 (6), 897–917.
You, L., Li, C., Liu, J.H., Huang, G.Z., 2011. Analysis on micro-geological causes of low-resistivity oil layers from Member 1 of Zhujiang Formation in Qionghai uplift. Glob. Geol. 30 (1), 65–70.
Zhang, L.K., Luo, X.R., Vasseur, G., Yu, C.H., Yang, W., Lei, Y.H., Song, C.P., Yu, L., Yan, J.Z., 2011a. Evaluation of geological factors in characterizing fault connectivity during hydrocarbon migration: application to the Bohai Bay Basin. Mar. Petrol. Geol. 28 (9).
Zhang, Y.C., Chen, Z.H., Li, X.S., Xu, X.D., Li, Q., 2011b. Petroleum accumulation characteristics and favourable exploration directions in Wenchang B Sag and its surrounding areas, Pearl River Mouth Basin. Petroleum Geology & Experiment 33 (3), 297–302.
Zhang, Y.C., Gan, J., Deng, Y., Wang, Z.F., Li, X.S., Chen, Z.H., 2009. Hydrocarbon plays in Wenchang B sag and its surrounding areas, the western Pearl River Mouth basin. China Offshore Oil Gas 21 (5), 303–307+312.
Zhang, Y.C., Gan, J., Li, H., 2013. Strike-slip deformation mechanism and its petroleum geology significance along south fault in Zhu III depression under extensional tectonic setting. China Offshore Oil Gas 25 (5), 9–15.
Zhang, Y.C., Zhang, K.K., Yuan, B., Li, H., 2014. Fault system and structural style of cenozoic and their controlling effects on hydrocarbon-forming in Wenchang sag. Sci. Technol. Eng. 14 (23), 26–31.
Zhang, Y.C., Zhu, W.L., Gao, Y.D., 2015. Late fault adjustment and late accumulation poll-forming model in Qionghai uplift, Pearl River Mouth Basin. Journal of Southwest Petroleum University (Science & Technology Edition) 37 (5), 55–63.
Zhong, Z.H., Liu, F., He, W.J., 2018. Sedimentary facies in Oligocene zhuhai member-2 in Wenchang sag and adjacent area, Pearl River Mouth Basin. Marine Origin Petroleum Geology 23 (3), 53–64.
Zhu, H.M., Li, L., Yang, W., 2013. Multi-azimuth seismic data applied analysis on the exploration and development of Wenchang sag. Prog. Geophys. 28 (5), 2587–2596.
Zhu, W., Mi, L., 2011. Atlas of Oil and Gas Basins, China Sea. Petroleum Industry Press, Beijing.